Point-by-point reply to reviews on manuscript "Experimental study on retardation of a heavy NAPL vapor in partially saturated porous media"

Anonymous Referee #1

Reference	Content
Point a)	**A revised introduction that provides a more compelling motivation for studying CS2 retardation and a more accurate framing of the experimental work to follow would allow readers to recognize what aspects of the work are novel and scientifically significant. For example, if CS2 retardation is really truly understudied (a quick search in a well established database revealed very few CS2 papers, which, coupled with its prevalence at NPL sites, surprised me) than say so. At several points in the paper, the authors refer to their experimental setup as "novel" (including conclusion #1), but basis of this claim is unclear; what exactly is novel about the setup and what processes/variables/systems does it open to investigation that were previously precluded?**
Reply	We have thoroughly revised the introduction incorporating recent research papers. We clarified the objective of our study, and improved the reasoning, in particular to show why studying retardation of CS2 is important. We are confident that the revised introduction will frame our experimental work more accurately and will be easier for readers to follow.
Point b)	**Conduct a saturated phase experiment to measure KD and, if not available in the literature, a surface tension experiment to measure KIW before excluding sorption at solid and interfacial phases from consideration.**
Reply	We have carefully consulted, among others, the papers indicated in your review and have come to the conclusion that sorption on the solid phase may be neglected based on the properties of the porous media and the physicochemical properties of CS2. A more detailed discussion is provided in Section 3.3 Retardation of CS2 on p. 19.
Point c)	**As appropriate, use parameters from (b) in your theoretical model of CS2 retardation to perform a more complete and rigorous process-based analysis of your experimental findings.**
Reply	See reply to Point b)
Point d)	**The significance of the dispersion/dispersivity parameters derived for CS2/the porous media is not clear to the reader. If you are going to perform this analysis, what is the important take-home for readers? As it stands, several of the conclusions are underwhelming – moments analysis works (conclusion #2), simple theoretical constructs from 1961 are imperfect (conclusion #3), diffusion effects increase with longer residence time (conclusion #4).**
Reply	We agree that the discussion of the dispersion/dispersivity parameters and the corresponding conclusions can be improved. We decided to shorten the discussion significantly and to focus on more important findings and conclusions concerning retardation and partitioning processes.
Point e)	**The conclusion most directly tied to the goal of the paper and potentially of greater interest to readers is #5, but suffers from interpretations based on assumptions of what processes control transport, since those processes were not specifically studied. The experiments and analysis suggested above in (a) would strengthen the conclusions that could be drawn.**
Reply	We have reconsidered our assumptions of which processes control transport, we

	carefully consulted relevant papers, and we incorporated a detailed discussion in ''Section 3.3 Retardation of CS2'' of our manuscript. We trust that the revised discussion of the partitioning processes improves the paper as a whole; moreover it supports the quality of the interpretation of our experimental results.
Point f)	**Conclusion #6 is potentially quite interesting, but needs more discussion and incorporation of more relevant literature. I accept that further experimental investigation of the biodegradation may lie beyond the scope of the current paper, but if the data are going to be presented at all, they should be discussed (e.g., the feasibility of anaerobic degradation to occur at such timescales; if CS2 is degraded so thoroughly so quickly (recoveries of only 1%!) then why has CS2 persisted at so many of the NPL sites for so long? etc.)**
Reply	We thank the reviewer for encouraging the discussion related to biodegradation of CS2. We have carefully consulted published studies which are all (except for Cox et al., 2013, see reference list in manuscript) concerned with waste-gas treatment plants using biofilters for manufacturing companies. They have found a small number of microbes capable of oxidizing CS2 in aerobic or anaerobic conditions. However, they also reported self-inhibitory effects with increasing CS2 concentrations. Hence, biodegradation of CS2 is only relevant in specific environments and under conditions which are most likely not met close to source zones at CS2-contaminated sites. We have incorporated the discussion at the end of ''Section 3.3 Retardation of CS2'' where the mass recovery is discussed; we also revised our conclusion. A comparison of our results with reported degradation rate constants from batch experiments was not feasible since effluent concentration measurements at the column outflow are the only available data and do not allow for calculations of rate constants.
Point g)	**Conclusion #7 is a bit disorganized, repeating some of #5 and #6 before recommending that SVE be used for CS2 remediation. This recommendation could be elaborated upon by discussion of what is actually being done and with what degree of success at the many NPL sites contaminated with CS2. Also, some caveat should be included, given that the volatility and rate of evaporation of CS2 liquid was not studied.**
Reply	We have revised the conclusion to improve our reasoning. SVE is the method of choice for the remediation of VOCs in the unsaturated zone and applies especially for CS2 given its physicochemical properties. Of course, SVE cannot be readily applied to the saturated zone when a spill of CS2 (DNAPL) reaches and penetrates the groundwater. It has to be combined with, for instance, steam injection or soil venting to actively vaporize contaminants.
Technical point a)	**If I understand the intended meaning correctly, “irreducible saturation” is more typically termed “residual saturation”.**
Reply	We generally used “irreducible“ for water and “residual” for NAPL. We now consistently use residual throughout the manuscript to avoid misunderstandings.
Technical point b)	**I didn’t understand the concept of filling the porous media columns “each with an overfill of around 30 cm”.**
Reply	The concept of filling the columns was rephrased to improve comprehensibility.
Technical point c)	**I found the schematic of the experimental system to be overly detailed to the point that it limited reader comprehension. I believe the He tank should be Ar instead? Several items in the figure weren’t in the legend. The purpose of the Tedlar bags was not clear. I would dramatically simply the figure.**
Reply	The flow chart of the experiment has been re-designed and simplified.
Technical point d)	**The rationale for bottom-up flow was never provided and seems to counter the stated motivation of examining density-driven flow.**
Reply	These experiments aimed at providing a basic understanding of vapor retardation with a clear differentiation from density-driven flow. Bottom-up flow was chosen since the injected vapor is heavier than soil air. Stable flow conditions (e.g. reduce fingering) could be ensured and additional influences (e.g. gravity) could be avoided. Density-driven flow

was investigated in an earlier experimental investigation.

Technical point e)	**The paragraph containing lines 1-10 on p 6 seemed particularly disorganized, jumping around from the N2 chase to the gas mixture, back to the chase.**
Reply	The paragraph has been revised and shortened.
Technical point f)	**Although 7 experiments are described (series 1-4 for glass beads; 1-3 for fine sand), only a fraction of these had full data – no saturation profiles for 3 of the 7; and poor mass recovery for series 3 fine sand. Because the saturation was at the heart of arguments regarding CS2 retardation, the missing saturation profiles for these experiments is noteworthy. That said, the accuracy of the saturation profiles was called into question on p 9. The validity of basing arguments on profiles that are simultaneous dismissed as misleading due to the small size of the tensiometers was confusing. Moreoever, column mass had been measurement throughout the experiment and supposedly provided an independent measure of moisture saturation that was more reliable. Why weren't these data shown instead of the tensiometer data (e.g., in Figure 3)? I don't mean to imply you should only show data you agree with, but if you fundamentally do believe that the tensiometer data are inaccurate, why present them to readers?**
Reply	We have revised the discussion about the water saturation profiles and tensiometer measurements since it was obviously prone to confusion. The missing water saturation profiles of Series 2 and 3 in fine glass beads are mentioned in the manuscript. We trust the tensiometer measurement at static conditions, but we question the measurement quality during active gas flow, especially with respect to the fluctuations measured. Since we monitored the total column mass by placing the entire set-up on a scale, we could assure that a drying-out of the porous medium was prevented. However, actually showing this data (basically a constant value) does not add to the manuscript. Hence, we decided to remove the right-hand graph of Figure 3 and only show the measured water saturation profiles.
Technical point g)	**As the authors note, it is not uncommon for compound-specific behavior to get lumped into dispersivity values, and also common for dispersivity values for nonreactive tracers to be considered more reliable. The authors might therefore consider using the non-reactive tracer data to arrive at a dispersivity value and fix this as an input parameter in the dispersion fitting of the CS2.**
Reply	Thank you for this suggestion. We did consider this approach and believe that it might give us a slightly different perspective, but overall, this will not improve the interpretation of our data.
Technical point h)	**The authors repeatedly mention grain-size distribution as a variable potentially influencing retardation. Presumably some of the grain-size effect is through its relationship to surface area (and therefore would affect solid-phase sorption and air-water interfacial accumulation). Some discussion and theoretical handling of the surface area impacts on retardation is needed.**
Reply	We have provided a detailed discussion in ''Section 3.3 Retardation of CS2'' related to the partitioning processes and their dependence on soil material and chemical compound properties. We are confident that the newly added information will improve our manuscript.

Anonymous Referee #2

Reference	Content
Point 1	**An important concern with this work is that, although in a gaseous state is 1.6 times denser that air, density effects have not been considered in the estimation of the retardation factor.**
Reply	Partitioning processes leading to retardation are not expected to be influenced by density effects, but vapor migration indeed is. Impact of density difference on vapor plume migration (advection) was investigated in a separate study (see Kleinknecht (2015) in reference list of manuscript). See also our reply to Technical Point d) above.
Point 2	**The authors must clearly describe the novel contributions of this study. Vapor retardation due to partitioning into the aqueous phase is an intuitive result.**
Reply	We have thoroughly revised our manuscript to highlight the novel contribution of our study. There are no experimental studies on retardation of CS2 vapor available. Hence, our study provides new data on this subject which also has been made available (see remark on data availability in manuscript).
Technical point 1	Page 1, line 10, "… as a function of porous medium …" is awkward.
Reply	Revised.
Technical point 2	The legend of Figure 1 is incomplete. Some of the apparatus are not listed.
Reply	Figure 1 has been re-designed and simplified.
Technical point 3	The are many repetitions in the manuscript. For example, the authors have mentioned several times throughout the manuscript that the experiments were conducted in two different porous media (fine glass beads and Geba fine sand) under both dry and partially saturated (moist) conditions.
Reply	We have carefully checked the manuscript and removed redundant phrases.
Technical point 4	The manuscript should be checked very carefully for grammatical errors. For example, (page 7, line 10) "an separate"; (page 7, line 29) insert "the" before "Henry's."
Reply	Thank you for bringing this to our attention.
Technical point 5	All symbols must be defined in the manuscript as soon as they appear. For example, none of the symbols in equation (1) have been defined.
Reply	We have checked the symbols and their correct definitions.
Technical point 6	The first sentence in the "Results and discussion" section does not belong there. It is more of introductory material.
Reply	Revised.
Technical point 7	Figure 9 deserves more attention. It is hard to follow.
Reply	We have removed the velocity-dependent symbol size and revised the entire section to facilitate reading.

List of relevant changes

1. Revision of abstract.
2. Revision of introduction.
3. Shortening and revision of section „Materials and methods“.
    1. Replaced Figure 1 by a simplified version of the flowchart.
    2. Included scanning electron microscopy images of porous media in „Materials and methods“.
4. Revision of section „Data evaluation“; including now theoretical approaches to estimate air-water interfacial adsorption.
5. Revision of section „Results and discussion“.
    1. Shortening of subsection „3.1 Water saturations“; removed right-hand side graph showing tensiometer recordings over time in Figure 4.
    2. Shortening of subsection „3.2 Impact of velocity on breakthrough“; removed Figure 6 and Figure 7.
    3. Major revision of subsection „3.3 Retardation of CS2“; added thorough discussion about partitioning processes and revised paragraph about biodegradation.
6. Major revision of conclusions including newly added insights.

Experimental study on retardation of a heavy NAPL vapor in partially saturated porous media

Simon M. Kleinknecht[1], Holger Class[2], and Jürgen Braun[1]

[1]Facility for Subsurface Remediation, Institute for Modelling Hydraulic and Environmental Systems, University of Stuttgart, Pfaffendwaldring 61, 70569 Stuttgart, Germany
[2]Department of Hydromechanics and Modelling of Hydrosystems, Institute for Modelling Hydraulic and Environmental Systems, University of Stuttgart, Pfaffendwaldring 61, 70569 Stuttgart, Germany

Correspondence to: Simon M. Kleinknecht (simon.kleinknecht@iws.uni-stuttgart.de)

This is a new or revised phrase.

~~This is a deleted phrase.~~

Abstract. NAPL contaminants introduced into the unsaturated zone spread as a liquid phase; however, they can also vaporize and migrate in a gaseous state. Vapor plumes migrate easily and, thus, pose a potential threat to underlying aquifers. ~~Heavy vapors preferentially migrate downward due to their greater density and, thus, pose a potential threat to underlying aquifers.~~ Large-scale column experiments were performed to quantify partitioning processes responsible for the retardation of carbon disulfide (CS_2) vapor in partially saturated porous media. The results were compared with a theoretical approach taking into account the partitioning into the aqueous phase as well as adsorption to the solid matrix and to the air–water interface. The experiments were conducted in large, vertical columns (i.d. = 0.109 m) of 2 m length packed with different porous media. A slug of CS_2 vapor and the conservative tracer argon was injected at the bottom of the column followed by a nitrogen chase. Different seepage velocities were applied to characterize the transport and to evaluate their impact on retardation. Concentrations of CS_2 and argon were measured at the top outlet of the column using two gas chromatographs. The temporal-moment analysis for step input was employed to evaluate concentration breakthrough curves and to quantify ~~diffusion/~~dispersion and retardation. The experiments conducted showed a pronounced retardation of CS_2 in moist porous media ~~as a function of porous medium and water saturation. An increase in the retardation coefficient with increasing water saturation was observed.~~ which increased with water saturation. The comparison with an analytical solution helped to identify the relative contributions of partitioning processes to retardation. Thus, the ~~vapor-retardation~~ experiments demonstrated that migrating CS_2 vapor is retarded as a result of partitioning processes ~~partitioning into the aqueous phase~~. Moreover, CS_2 dissolved in the bulk water is amenable to biodegradation. First evidence of CS_2 decay by biodegradation was found in the experiments. The findings contribute to the understanding of vapor plume transport in the unsaturated zone and provide valuable experimental data for the transfer to field-like conditions.

1 Introduction

Subsurface contamination is a major concern in industrialized as well as in developing and emerging countries. NAPL contaminants introduced into the unsaturated zone spread as a liquid phase; however, they can also vaporize and migrate in a gaseous state. In particular, vapor (gas) plumes migrate easily in the unsaturated zone (Barber and Davis, 1991; Davis et al., 2005, 2009; Höhener et al., 2006; Brusseau et al., 2013). ~~Vapors heavier than air preferentially migrate downward, posing a potential threat to aquifers.~~ When assessing the danger of groundwater contamination by downward-migrating vapor plumes, retention effects on transport are of major interest. Processes such as dissolution into the bulk water or adsorption at interfaces ~~partitioning to bulk water or adsorption on sand grains~~ affect the migration of vapors in the unsaturated zone. Vapor retardation could potentially slow down migration and reduce the total contaminant mass eventually reaching, and thus endangering the groundwater. While fate and transport of vapor plumes have attracted a great deal of attention over the past years, further (contaminant-specific) investigations are necessary to improve the process understanding required to assess the threat to the environment (Rivett et al., 2011).

~~The contaminant used in this work was~~ Carbon disulfide (CS_2) is a toxic, industrial, non-polar solvent among others used to manufacture viscose rayon. ~~It is highly volatile and characterized by a very high density (1.6 times the air density) in a gaseous state~~. It is a dense non-aqueous phase liquid and highly volatile at standard conditions. Its vapor is characterized by a high density (1.6 times the air density) and is explosive. Hence, CS_2 vapor can migrate in the unsaturated zone, intrude into buildings, and distant ignition is possible. ~~CS_2 has been found in 139 (11.2 %) contaminated sites on the U.S. EPA National Priority List (NPL), according to McGeough et al. (2007).~~ The U.S. Agency for Toxic Substances and Disease Registry ranks CS_2 168th on the Substance Priority List (SPL) of hazardous substances found on U.S. EPA National Priority List (NPL) sites (ATSDR, 2015). CS_2 has been found in 122 of the 1,844 sites on the NPL (USEPA, 2016). In addition, CS_2 has also been detected on CCl_4-contaminated sites as a result of abiotic degradation of CCl_4 (Davis et al., 2003).

Experimental studies (e.g. Brusseau et al., 1997; Kim et al., 1998; Costanza-Robinson et al., 2013) have been conducted to investigate retardation of the most common VOC in unsaturated porous media using short columns in the range of few decimeters and high flow velocities. Experimental results have been compared with standard as well as advanced advection-dispersion models (Popovičová and Brusseau, 1998; Toride et al., 2003). Corley et al. (1996) showed that low concentrations of volatile organic compounds distribute in the bulk phases (air, water and solid), adsorb to the air–water interface, and partition into intraparticle pores in unsaturated and saturated porous media. ~~While it has been demonstrated in experiments that the gas-water interface poses a high potential for retardation (Brusseau et al., 1997), determining the size of interfacial areas and partitioning parameters in theoretical approaches is considered a challenge (Hoff et al., 1993; Kim et al., 1997, 1998).~~ While it has been demonstrated in experiments that the gas-water interface poses a high potential for retardation (Brusseau et al., 1997; Costanza-Robinson and Brusseau, 2002b), determining the effective interfacial area, which controls the contaminant mass transfer, is still subject of intensive research (Goss, 2009; Kibbey and Chen, 2012; Brusseau et al., 2015). Mayes et al. (2003) stated that immobile water in pores could act as a short-term sink and as a long-term source of potential contaminants. The effect of moisture content on vapor retention has also been described by Cabbar and Bostanci (2001) and Maxfield et al. (2005) who

discovered retardation to be negatively correlated to water saturation due to preferred adsorption on the solid matrix of certain components. The latter has additionally shown the dependency of retardation on the properties of the chemical ~~compound~~ component of interest. For instance, noble gases show no retardation at all. In summary, retardation of a contaminant vapor is a combination of different partitioning processes; their relative contribution depends on the physicochemical properties of the ~~compound~~ component as well as the properties of the porous medium (Costanza-Robinson et al., 2013).

~~This component and water-saturation-dependent~~ The component- and porous-medium-dependent behavior of gas-phase retention emphasizes the need for a thorough investigation into retardation of carbon disulfide (CS_2) in partially saturated porous media. No detailed experimental studies on the retardation behavior of CS_2 vapor are available. Therefore, the first objective of this study was to design and conduct a large-scale column experiment ~~were designed and conducted~~ to quantify retardation of CS_2 with clearly-defined and controlled boundary conditions. The experiments were conducted in vertical columns (i.d. = 0.109 m) of 2 m length packed with a porous medium. They were carried out under dry conditions and at static water saturations. Reproducible water saturations (initial conditions) were obtained by saturation with water and subsequent drainage under controlled conditions at predetermined capillary pressures. Tensiometers installed along the column were used to derive water-saturation profiles. A ~~finite slug containing gaseous~~ slug of CS_2 vapor ~~as well as~~ and a non-retarding, conservative tracer (argon) was injected via an injection section at the bottom of the column. Velocities were varied in the range 25 to 200 cm h^{-1} in different experiments. Effluent concentrations of CS_2 and argon were measured online with gas chromatographs at the top outlet of the column. ~~Tensiometers installed along the column measured capillary pressures to monitor the drainage process and to obtain water-saturation profiles. Gas flow rates were controlled by mass-flow controllers and additionally measured by a bubble flow meter.~~ This set-up enabled for the quantification of CS_2 retardation as a function of porous medium, water saturation, and velocity. The second objective was to compare the experimental results with a theoretical approach, taking into account the different partitioning domains available for CS_2 and eventually responsible for retardation. This allowed to quantify contributions of the partitioning processes to total retardation. Hence, fundamental knowledge regarding the potential to delay or prevent a contamination of an underlying aquifer was gained.

2 Materials and methods

~~This work focused on the experimental investigation into the retardation of CS_2 vapor in partially saturated porous media. This section addresses the experimental set-up, the procedures, and data evaluation methods used in this study. Table 2 shows the physicochemical properties of the contaminant carbon disulfide (CS_2) at 20°C, 1013.15 hPa.~~

2.1 Experimental set-up

The experiments were conducted in vertical, stainless steel columns of 2 m length packed with two different types of porous media (Figure 1). The column (length = 2 m, i.d. = 0.109m) consisted of two custom-built, 1 m long sections. The ports along the column at a distance of 25 cm allowed for the installation of tensiometers to monitor capillary pressures. At the bottom of the column, the injection section with a base plate was installed. Into this base plate, a porous plate made of recrystallized

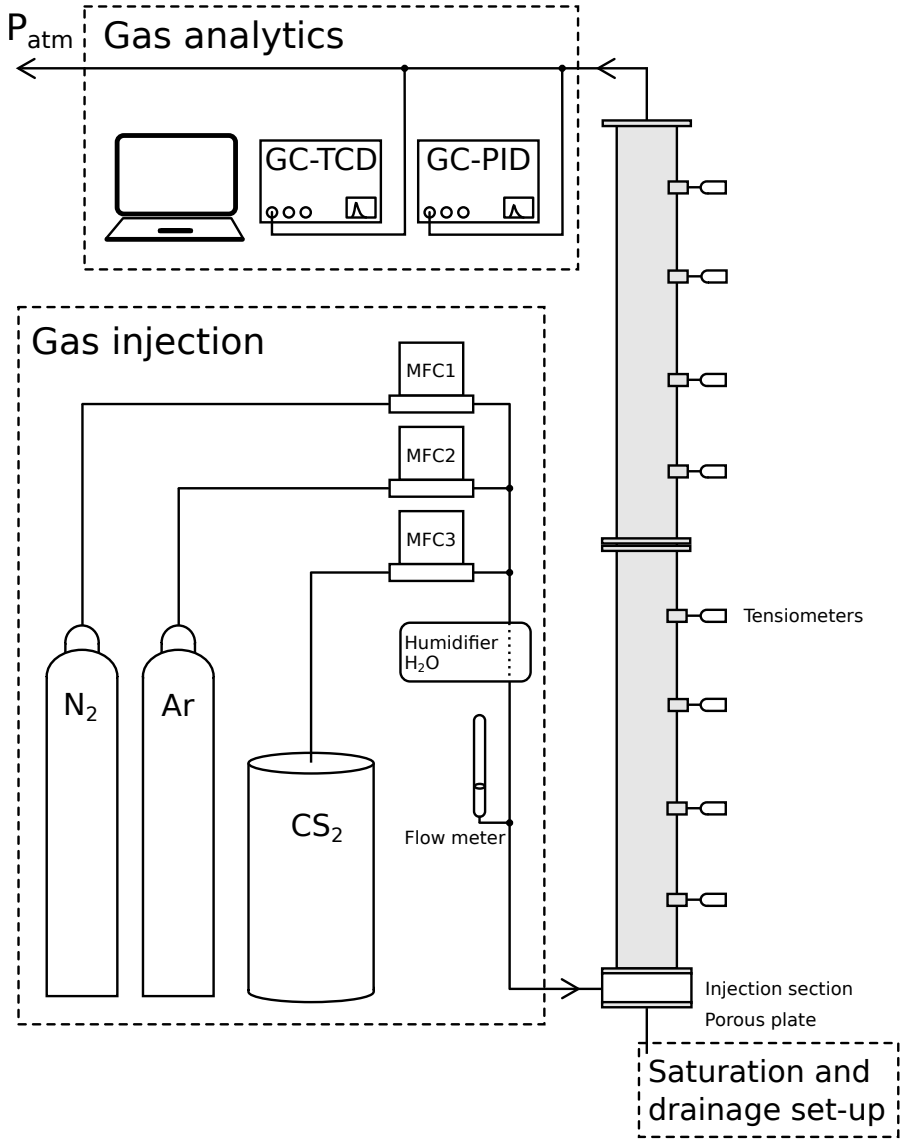

Figure 1. Flowchart of vapor-retardation experiment showing column, injection and saturation/drainage set-up.

silicon carbide was glued to act as a suction plate for the water drainage. The bottom of the column was realized as a constant-mass-flux boundary while the top is open to the surroundings, hence, at constant pressure.

Two different types of porous media (Table 1) were used in the experiments: fine glass beads (soda-lime glass, Sigmund Lindner, Warmensteinach, Germany) and Geba fine sand (Quarzsande GmbH, Eferding, Austria). Their grain-size distributions as well as capillary pressure - water saturation relationships are shown in Figure 2. Figure 3 shows scanning electron microscopy images of both materials illustrating their different shape and surface roughness. The columns were packed by

Table 1. Characteristic properties of the porous media used for the experiments.

Parameter	Fine glass beads	Geba fine sand
Bulk density, kg m^{-3}	1420	1390
Grain size, mm	0.1 – 0.2	0.06 – 0.35
Permeability, m^2	$1{\cdot}10^{-11}$	$1{\cdot}10^{-11}$
Grain diameter d_{50}, µm	162	140
Pore diameter (median), µm	66	39
Smooth-sphere assumption SA, cm^{-1}	22.8	24.3
van Genuchten (constrained)		
α, cm^{-1}	0.0193	0.0145
n, dimensionless	17.783	10.305
θ_s, cm^3 cm^{-3}	0.392	0.460
θ_r, cm^3 cm^{-3}	0.043	0.071

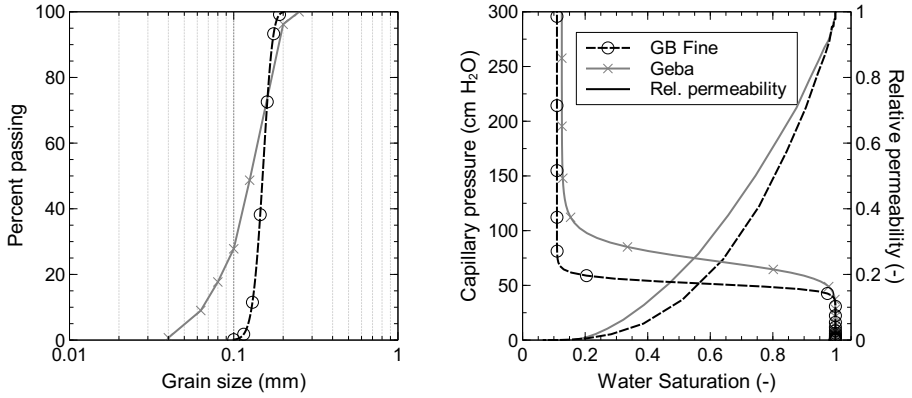

Figure 2. Grains-size distribution, capillary pressure–saturation relationship, and relative permeabilities (for the wetting phase) of materials used in experiments.

dry pluviation using a sand rainer (Rad and Tumay, 1987; Lagioia et al., 2006). ~~The design of the rainer was adopted from Rad and Tumay (1987) with modifications according to Lagioia et al. (2006). The columns consisting of two column sections were filled section after section, each with an overfill of around 30 cm. This prevented additional layering of the porous medium.~~ This ensured a homogeneous porous medium throughout. The columns were sealed with cover plates equipped with 1/8" tube fittings (SS-6M0-1-4RT, Swagelok). The experiments were carried out under dry conditions as well as at ~~irreducible~~ residual, static water saturation. Comparable initial conditions for each experiment were guaranteed by a set-up controlling and monitoring saturation and drainage. The drainage of the porous media was realized by means of the porous plate at the bottom of the column exclusively permeable for water when fully saturated. This allowed for setting the water Table lower than the

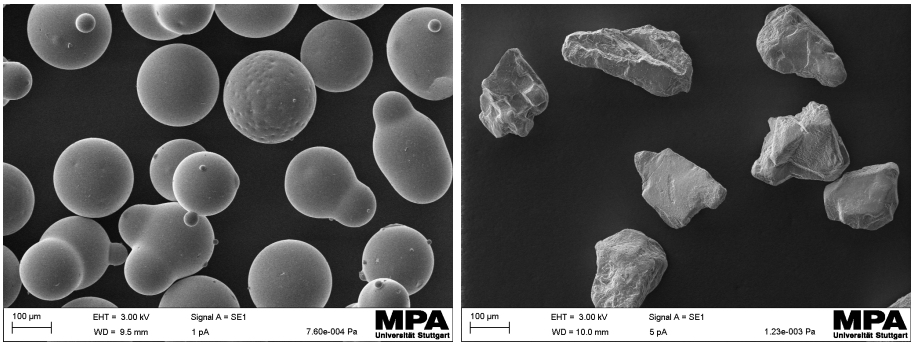

Figure 3. Scanning electron microscopy images of fine glass beads (left) and Geba fine sand (right) at a scale of 100 µm.

Table 2. Physicochemical properties of contaminant carbon disulfide (CS_2) at 20°C, 1013.15 hPa.

Parameter	Value	Reference
CAS number	75-15-0	
Molecular weight (M_{CS2}), g mol^{-1}	76.1	Budavari (1996)
Density of liquid (ρ), kg m^{-1}	1263	Budavari (1996)
Solubility in water ($c_{w,sat}$), g L^{-1}	2.1	Riddick et al. (1986)
Henry constant (H_{cc}), dimensionless	1.04	Lide (2005)
Octanol-water partitioning coefficient ($log(K_{OW})$), dimensionless	2.00	USEPA, 1996
Organic-carbon partitioning coefficient (K_{OC}), L kg^{-1}	45.7	USEPA, 1996
Air–water partitioning coefficient (K_{IA}), cm	6.87 x 10^{-6}	Valsaraj (1988)
Boiling point (T_B), °C	46.5	Budavari (1996)
Vapor pressure (P_{sat}), hPa	396.9	Wagner equation
Saturation concentration in gas phase ($c_{a,sat}$), kg m^{-3}	1.239	Ideal gas law
Diffusion coefficient in air (D_{CS_2Air}), cm^2 s^{-1}	9.71 x 10^{-2}	Chapman-Enskog

bottom of the column or flume. The saturations followed the capillary pressure–saturation relationship (Fig. 2) measured in the laboratory. The water saturation was monitored using the tensiometers installed at the column ports. The tensiometer used for measuring capillary pressures consisted of a ceramic frit (length = 8 mm, o.d. = 6.5 mm, pore size = 2.5 um, porosity = 45 %, Porous Ceramics, Soilmoisture Equipment Corp., Santa Barbara, USA) glued in a stainless steel capillary (length = 200 mm, o.d. = 6 mm, i.d. = 4 mm). In addition, the column was placed on a scale to permanently monitor its weight and thus the total amount of water.

The injection section at the bottom of the column allowed for the injection of a gas-mixture slug at a predefined mass flux and, in addition, for a controlled upward flow stabilizing the vapor front. The CS_2 vapor was prepared prior to injection. Table 2 shows the physicochemical properties of the contaminant carbon disulfide (CS_2) at 20°C, 1013.15 hPa. A predefined amount

of liquid CS_2 was injected into a barrel ($V = 50\,L$) and pressurized to an excess pressure of about 2 bar with nitrogen to ensure defined vapor properties. The tracer argon was provided from a gas cylinder (Westfalen AG, Münster, Germany). Constant mass fluxes of the injected CS_2 vapor and of the conservative tracer argon were critical to the experiment. Mass fluxes of argon, CS_2 vapor, and nitrogen were controlled by mass-flow controllers (EL-FLOW, $Q_{max} = 3$, 50, and $10\,mL\,m^{-1}$, Bronkhorst High-Tech B.V., Ruurlo, Netherlands). Complete gas tightness of the entire set-up was ensured by using 1/8" stainless steel capillaries throughout. The slug of the gas mixture (CS_2, argon ($Q_{Ar}/Q_{total} = 1.4\,\%$), and carrier nitrogen) was injected and then pushed through the column using a nitrogen chase at the same flow rate. ~~Prior to injection into the column, argon (approximately $Q_{Ar}/Q_{total} = 1.4\,\%$) was added to the total flow. The mass balance was closed based on the measured flow rate, and the injection and effluent concentrations. The second objective of the nitrogen chase was to observe the recovery of the contaminant and reversibility of partitioning processes.~~ The nitrogen chase allowed to observe the contaminant recovery and the reversibility of partitioning processes.

In the case of moist experiments, the gas mixture slug was humidified with ultra-pure water (RH = 100 %) to avoid a drying-up of the moist porous medium. For the preparation of the gas-mixture slug, a custom-built miniature vaporizer (ICTV, University of Stuttgart, Germany) with an ultra-low volume pump (M6, VICI AG International, Schenkon, Switzerland) was used. The nitrogen used for the chase was bubbled through a gas scrubber filled with ultra-pure water. The inlet steel capillary loop (length = 4 m) and the scrubber were placed in a temperature-controlled water bath (Ministat 125, Huber Kältemaschinenbau GmbH, Germany) to minimize temperature-induced fluctuations during the experiments. The mass balance was closed based on the flow rate measured at the inflow, and the injection and effluent concentrations.

In the column outflow, CS_2 and argon concentration were measured to quantify retardation in dry and moist porous media. Two gas chromatographs were directly connected in-line to the column outlet. CS_2 concentrations were determined using a gas chromatograph with a photoionization detector (GC-PID HE1, Meta Messtechnische Systeme GmbH, Dresden, Germany) and argon concentrations were determined using a gas chromatograph with thermal conductivity detector (GC-TCD, Multiple gas analyzer 8610-0270, SRI Instruments Europe GmbH, Bad Honnef, Germany). Single-point calibrations were conducted prior to and after each run. Measurement intervals were set depending on the flow velocity such that a high temporal resolution (0.021 to 0.065 PV) of the breakthrough curves was obtained. Prior to the start of the slug injection, the concentration of CS_2 and argon in the slug mixture was measured as a base to normalize concentrations. A relative pressure transducer connected to the column inlet before the injection section was used to monitor the injection pressure. Since the top column outlet was open to the atmosphere (P_{atm}), this corresponded to the pressure loss caused by the flow through the porous medium. Temperature sensors and absolute pressure transducer continuously measured and recorded ambient and water bath temperature as well as atmospheric pressure in the vicinity of the experiment.

2.2 Experimental procedure

Various experiment series were conducted in two different porous media (fine glass beads and Geba fine sand) under both dry and partially saturated (moist) conditions. Within each series the columns were not repacked and no saturation-and-drainage cycle (SD) was carried out since first tests proved that the partitioning processes were fully reversible. The water saturation

or total amount of water was monitored throughout the experiment. The slug of the gas mixture was injected with a predefined mass flux into the bottom of the 2 m long column such that it resulted in the designed seepage velocity. In each series, experiments were performed with different velocities including 25, 50, 100, and 200 $\mathrm{cm\,h^{-1}}$ (approx. 0.125, 0.25, 0.5, and 1.0 $\mathrm{PV\,h^{-1}}$) to observe kinetic effects on retardation. A slug of about 3.5 PV was used which corresponded to injection durations of approx. 3.5, 7, 14, and 28 h depending on the respective velocities. This ensured a residence time (plus safety factor) sufficient to attain steady-state conditions and for partitioning processes to reach equilibrium.

The experiments were conducted in four steps. In the first step, the flow rates (slug and chase) were adjusted to match the target seepage velocity. In the second step, the column was flushed with nitrogen. While maintaining constant flux, the inflow was switched to the slug injection of the gas mixture in the third step. After injecting 3.5 PV it was switched back to the nitrogen chase (fourth step).

2.3 Data evaluation

~~The objective of the experiments was to quantify the retardation of CS_2 vapor.~~ The quantification of retardation was based on gas concentration measurements of CS_2 and argon. Possible influences on the determined retardation factors due to experimental artifacts such as a deviation between theoretical and actual gas-effective pore volume had to be taken into consideration. Hence, for each experiment the breakthrough curve of CS_2 was related to that of argon. Concentrations were normalized with respect to the steady-state concentrations ($c = c_{exp}/c_{ss}$). Mass balance was calculated from concentration data and measured gas flow rates. Data was evaluated based on elapsed time and then correlated via flow rate, resulting from mass flux, to gas-effective pore volume. ~~Moreover, both the slug itself and the nitrogen chase were considered which allowed for a separate evaluation of the slug front and tail (front of nitrogen chase).~~ Breakthrough curves were evaluated using the temporal-moment analysis (TMA) for a step input (slug) as proposed by Yu et al. (1999) and Luo et al. (2006). The advantage of TMA "is that no underlying physical model is needed for calculating the travel times" (Yu et al. (1999), p. 3571), and the breakthrough curves of the CS_2-Ar mixture (slug front) as well as the nitrogen chase (slug tail) can be evaluated individually. ~~Moreover, TMA can also be applied to asymmetrical BTCs resulting from non-equilibrium sorption processes during transport. Hence, retardation of CS_2 in moist and dry porous media could be compared and the impact of water saturation on retardation of CS_2 could be delineated.~~

TMA was applied to obtain transport parameters (seepage velocity [Eq. A9] and dispersion coefficient [Eq. A10]) and mean breakthrough arrival (Eq. A7) time from concentration breakthrough curves. The retardation factor R of CS_2 vapor was calculated from the ratio of the respective moments or mean breakthrough arrival time.

$$R = \frac{\tau_{CS_2}}{\tau_{Ar}} = \frac{M_{1,CS_2}}{M_{1,Ar}} \tag{1}$$

This ensured the independence from experimentally-induced deviations and thus allowed to delineate the impact of water saturation and velocity on retardation.

~~Experimental retardation factors were compared with a theoretical factor. Brusseau et al. (1997) used carbon dioxide (CO_2) as a tracer whose predominant source of retardation was the partitioning into the aqueous phase. The similarity of CS_2 and CO_2 regarding solubility in water and Henry constant suggests a comparable retardation behavior for CS_2. Hence, partitioning~~

~~into the aqueous phase is considered the only contribution. Adsorption on grains (3) and at the gas-water interface (4) (terms on the right hand-side of Eq. 2) will be neglected. This then yields the adapted theoretical retardation coefficient.~~ Retardation of a component can be estimated using analytical solutions based on experimental parameters and component-dependent coefficients for the different partitioning domains. Brusseau et al. (1997) showed that the theoretical retardation coefficient of a gaseous component in the unsaturated zone can be calculated with

$$R_t = 1 + \beta_w + \beta_s + \beta_{IA} = 1 + \frac{\theta_w}{\theta_a K_H} + \frac{\rho_b K_D}{\theta_a K_H} + \frac{K_{IA} A_{IA}}{\theta_a} \tag{2}$$

~~where θ_w is volumetric water content, θ_a is gas-filled porosity, K_H (dimensionless) is Henry's constant.~~ where θ_w is volumetric water content, θ_a is gas-filled porosity, K_H (dimensionless) is the Henry's constant, K_D ($\mathrm{cm^3\,g^{-1}}$) is the sorption coefficient for water-saturated conditions, ρ_b ($\mathrm{g\,cm^{-3}}$) is the dry soil bulk density, K_{IA} (cm) is the adsorption coefficient at the gas-water interface, and A_{IA} ($\mathrm{cm^2\,cm^{-3}}$) is the specific surface area of the gas-water interface.

The coefficient K_D for CS_2 can be estimated with

$$K_D = K_{OC} \times f_{OC} \tag{3}$$

where K_{OC} ($\mathrm{L\,kg^{-1}}$) is the soil organic carbon partitioning coefficient and f_{OC} is the fraction of organic carbon in the soil material. The air–water partitioning coefficient K_{IA} of CS_2 can be estimated using empirical correlations between the interfacial-water partitioning constant K_{IW} and the octanol–water partitioning coefficient K_{OW} (Valsaraj, 1988).

$$K_{IW} = 3 \times 10^{-7} K_{OW}^{0.68} \tag{4}$$

$$K_{IA} = \frac{K_{IW}}{K_H} \tag{5}$$

The air–water interfacial area can be estimated with a correlation found by Costanza-Robinson et al. (2008) based on X-ray microtomography measurements of glass beads and natural sands.

$$A_{IA} = SA[(-0.9112)S_w + 0.9031] \tag{6}$$

where SA is the geometric surface area according to the smooth-sphere assumption (Tab. 1) and S_w is the water saturation.

3 Results and discussion

Column experiments were conducted with dry and moist porous media to characterize retardation of CS_2 vapor. Table 3 shows the experimental conditions of each series performed in fine glass beads and Geba fine sand. Several series of experiments were performed in each porous medium to quantify retardation. Series 1 refers to the experiments conducted in dry porous media while Series 2 to 4 refer to the experiments in moist conditions. A saturation-and-drainage cycle was performed prior to each moist series. A slug of 3.5 PV of the gas mixture was injected ensuring, even for high flow rates, a sufficient residence time to

Table 3. Experimental conditions of vapor-retardation experiments in fine glass beads and Geba fine sand in dry and moist conditions (series).

Series	1	2	3	4
Condition	dry	moist	moist	moist
		Fine glass beads		
Porosity (ϕ)	0.40	0.40	0.40	0.40
Mean water saturation (S_w)	0.0	0.088	0.154	0.073
Eff. pore volume, L	7.72	7.04	6.53	7.16
		Geba fine sand		
Porosity (ϕ)	0.40	0.40	0.40	-
Mean water saturation (S_w)	0.0	0.162	0.150	-
Eff. pore volume, L	7.58	6.35	6.45	-

reach equilibrium in the 2 m long column. Different velocities (25, 50, 100, and 200 $\mathrm{cm\,h^{-1}}$) were applied, based on previously conducted experiments investigating density-driven vapor migration (Kleinknecht et al., 2015). Breakthrough curves under the prevailing experimental conditions were determined from concentration measurements at the column outlet. The temporal-moment analysis (Sec. 2.3) was applied to the breakthrough curves (BTC) to quantify diffusion/dispersion and retardation as a function of the porous media, the water saturation, and the flow conditions. A detailed summary of all experiments (experimental conditions, injected mass, and mass recovery) is given in Tables 5 and 6 in the appendix.

3.1 Water saturations

The moist porous medium required for this investigation was obtained by saturation and subsequent drainage via a suction plate. ~~The suction applied at the bottom of the column during drainage was responsible for the observed water saturation profiles.~~ The capillary pressure was measured with tensiometers installed at the column ports to derive water saturations along the column (P_c–S_w, Fig. 2). Mean water saturations of the moist series are given in Table 3.

Figure 4 ~~(left-hand)~~ shows the initial water saturation profiles along the column measured in fine glass beads (only Series 4) and Geba fine sand (Series 2 and 3). Unfortunately, no tensiometer measurement data was available for Series 2 and 3 in fine glass beads. Thus the missing profiles have to be considered an element of uncertainty when evaluating retardation of CS_2 of these series. However, the available profile of Series 4 revealed a uniform saturation along the column, only slightly increasing toward the bottom from $S_w = 0.07$ to 0.14. The very narrow and uniform grain-size distribution of the fine glass beads was responsible for a sharp transition from full to ~~irreducible~~ residual saturation (see P_c–S_w curve in Fig. 2), thus favoring a uniform saturation profile. In Geba fine sand, a constant water saturation of $S_w = 0.15$ above a column height of 70 cm was measured. However, both profiles showed a pronounced increase in the water saturation toward the bottom of the column, apparently reaching fully-saturated conditions according to the P_c–S_w relationship of Geba fine sand (Fig. 2). Still, capillary pressures of $P_c = 55$ and 65 hPa were measured at the lowest port. The suction applied via the porous plate was limited by its air

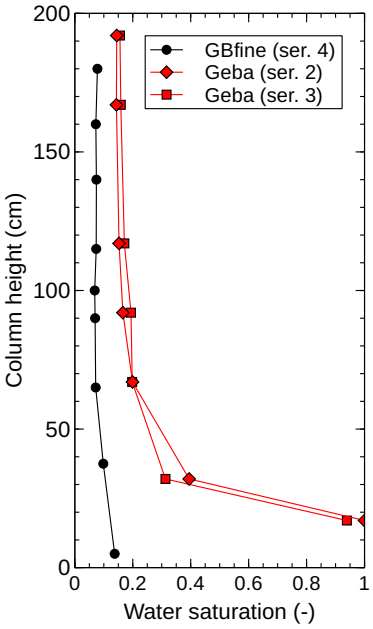

Figure 4. Initial water saturation ~~and progression of water saturation in experiment with Geba fine sand (Series 2)~~.

entry pressure. A further decrease of pressure would have resulted in a breakthrough of air (continuous gas phase). The mean water saturation (Table 3) but also the observed profiles were expected to have an impact on the retardation behavior of CS_2, as discussed in Sec. 3.3. ~~Figure 4 (right-hand) shows an exemplary progression of water saturations measured in Experiment 28 of Series 2 with Geba fine sand (Table 6). The saturations were based on tensiometers along the column during the injection of the slug and the subsequent nitrogen chase. The tensiometers suggested an apparent change in water saturation during active gas flow through the porous medium. This was most likely provoked by the pressure increase due to the injection and the gas flow around the tensiometer. It is important to note that the tensiometers measured the suction at a very spatially-limited location in the porous medium due to the small size of their tips (o.d. = 6 mm, length = 8 mm). In addition, the pressure transducers of the tensiometers showed periodic fluctuations as a result of daily temperature changes in the laboratory hall and due to varying ambient pressure.~~

~~A drying-out of the porous medium was prevented~~ A constant water-saturation profile in the porous medium was ensured by the humidification of all gases (gas-mixture slug and nitrogen chase) prior to injection. This was confirmed by ~~the water mass balance by means of the~~ a continuous weight measurement of the entire column throughout all experiments conducted within a series. Hence, the initial water-saturation profile could be maintained ~~throughout~~ during the experiments. ~~These experiments allowed for the characterization of transport behavior under different initial and controlled boundary conditions.~~

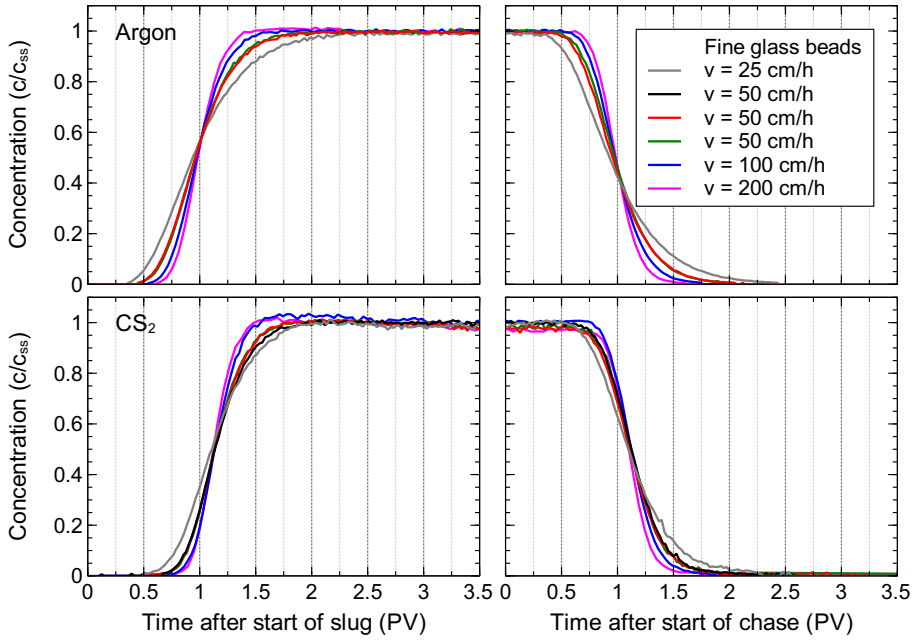

Figure 5. Breakthrough curves of CS_2 and Ar in moist fine glass beads ($S_w = 0.088$) for different velocities.

3.2 Impact of velocity on breakthrough

~~The impact of the velocity on the concentration breakthroughs of argon and CS_2 was investigated. Thus, different seepage velocities were applied to characterize the transport.~~ Different migration velocities were applied to study their impact on the transport of argon and CS_2. Figure 5 ~~and 6~~ shows breakthrough curves of CS_2 and argon as a function of pore volume for different flow conditions (velocities) in moist fine glass beads. ~~and Geba fine sand.~~ The breakthrough curves were adapted to the actual gas-effective pore volume determined from the mean breakthrough arrival time τ_{Ar} (Eq. A7) of the conservative tracer argon. Seepage velocities of about 25, 50, 100, and 200 $\mathrm{cm\,h^{-1}}$ (residence time of about 8, 4, 2, and 1 h) were applied successively in the same column and under similar initial conditions. The lines represent measured concentrations (c/c_{ss}) normalized to steady-state concentration. The graphs are split and the right-hand side shows the outflow concentrations after the injection was switched from the gas-mixture slug to the nitrogen chase. ~~Thus, these experiments allowed for the individual evaluation of the slug and of the nitrogen chase breakthroughs.~~ The skewness of a BTC is a result of the longitudinal molecular diffusion and the mechanical mixing. The BTCs of argon and CS_2 shown in the graphs illustrate that the skewness increased with decreasing seepage velocity as a result of ~~increased~~ diffusion during the longer residence time. ~~Since argon was used as a conservative tracer, its breakthrough was a function of the seepage velocity only. CS_2 was additionally affected by retardation partitioning processes, hence its breakthrough depended on seepage velocity as well as water saturation. The retardation of CS_2 is discussed in detail in the following Section 3.3. The repetitions with a velocity of about 50 $\mathrm{cm\,h^{-1}}$ proved that equilibrium was reached and they showed good reproducibility of the experiments.~~

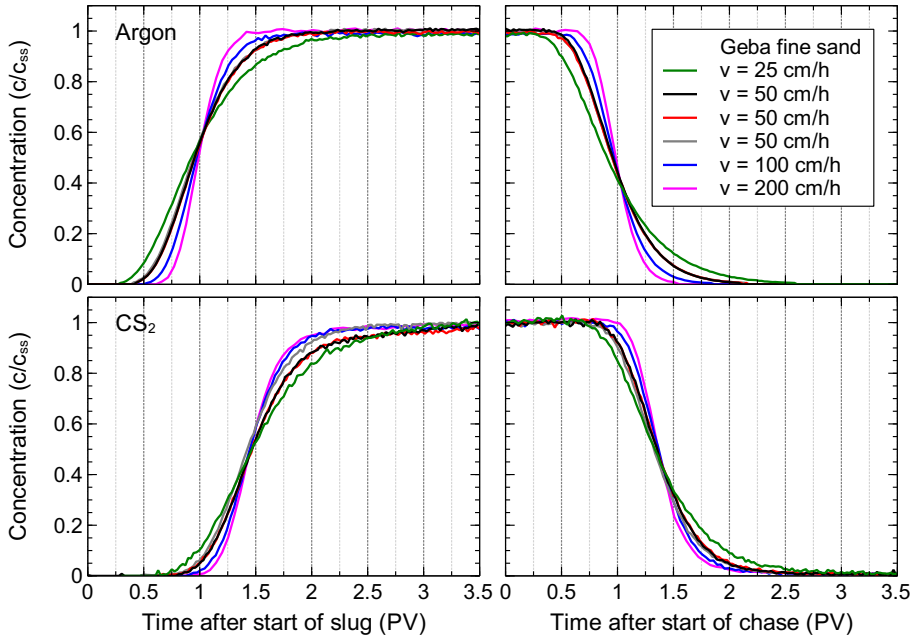

Figure 6. ~~Breakthrough curves of CS_2 and Ar in moist Geba fine sand ($S_w = 0.15$) for different velocities.~~ **Figure removed in revised manuscript!**

~~The BTCs were evaluated with the temporal-moment analysis (TMA, see Sec. A3) to obtain dispersion coefficients (Eq. A10) of argon and CS_2 for different flow conditions.~~ Dispersion coefficients were determined from temporal-moment analysis (TMA, see Sec. A3) of the breakthrough curves. ~~Figure 7 shows dispersion coefficients as a function of velocity of these experiments in moist porous media.~~ Dispersion coefficients of argon and CS_2 increased from $D_{Ar} = 0.089$ to $0.142\,\mathrm{cm^2\,s^{-1}}$ and $D_{CS_2} = 0.033$ to $0.074\,\mathrm{cm^2\,s^{-1}}$ as a function of the seepage velocity ~~and the porous medium~~. ~~The dispersion coefficient is defined as $D = D^* + \alpha v$ (Eq. A5).~~ Under static conditions ($v = 0\,\mathrm{cm\,h^{-1}}$), the effective binary diffusion coefficients D^* in porous media should apply. ~~D^* is defined as the product of the binary diffusion coefficient (Eq. A1) of the component in nitrogen and a tortuosity factor (Eq. A4). In the case of flow, the dispersion coefficient increases due to mechanical mixing which is a measure of the heterogeneity of the porous medium or the flow region, respectively. It is defined as the product of dispersivity α and velocity.~~ The effective binary diffusion coefficients D^* and the dispersivity α were determined based on ~~the breakthrough curves of the experiments. Based on the equation above,~~ a linear regression ~~was~~ fitted to the dispersion coefficients as a function of the velocity for each porous medium. The y-intercepts of the regression lines represent the coefficient D^* and the slopes express dispersivity α of the respective porous medium. The theoretical coefficient D_t^* was determined according to the Chapman-Enskog theory and the approach by Millington and Quirk (1961) which accounts for tortuosity due to porous matrix and water saturation (see Sec. A1). Table 4 compares theoretical with experimental effective binary diffusion coefficients of CS_2 and argon in fine glass beads and Geba fine sand under the given experimental conditions (water satu-

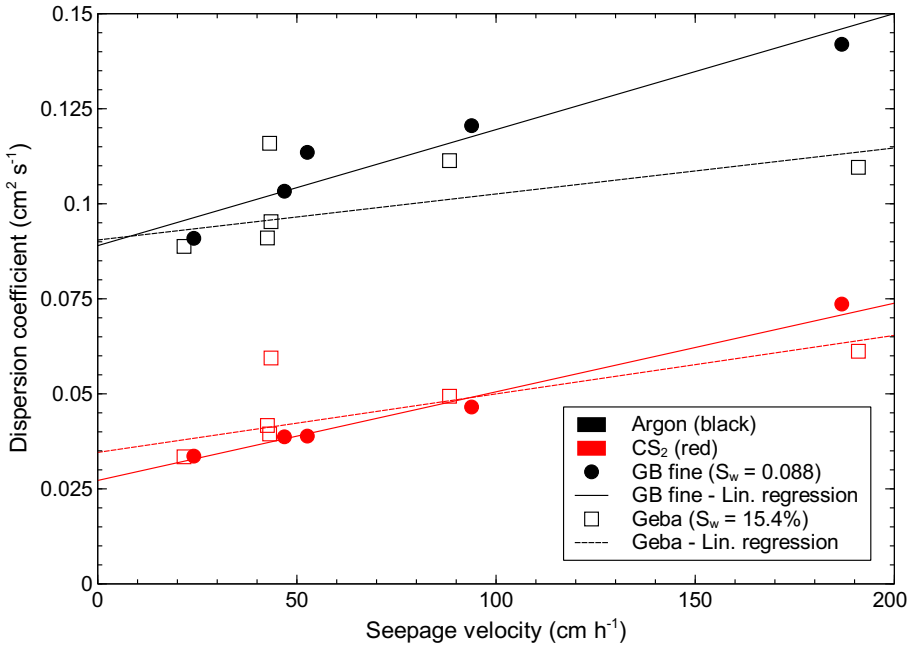

Figure 7. ~~Dispersion coefficients of CS_2 and Ar determined from TMA as a function of velocity. Experiments were conducted in fine glass beads ($S_w = 0.088$, Series 2) and Geba fine sand ($S_w = 0.162$, Series 2).~~ **Figure removed in revised manuscript!**

Table 4. Theoretical and experimental effective binary diffusion coefficient D^* of argon and CS_2, dispersivity α, and coefficient of determination R^2 of linear regression determined from experiments in moist porous media (Series 2).

Porous medium		Fine glass beads	Geba fine sand
Water saturation S_w		0.088	0.162
Tortuosity τ		0.220	0.161
Argon	D_t^*, $cm^2\ s^{-1}$	0.0386	0.0284
	D^*, $cm^2\ s^{-1}$	0.0909	0.0966
	α, cm	1.029	0.313
	R^2 (lin. regression)	0.919	0.254
CS_2	D_t^*, $cm^2\ s^{-1}$	0.0213	0.0157
	D^*, $cm^2\ s^{-1}$	0.0263	0.0332
	α, cm	0.888	0.552
	R^2 (lin. regression)	0.987	0.952

ration S_w and tortuosity τ). ~~In fine glass beads, effective binary diffusion coefficients of argon were $D^*_{Ar} = 0.0909\,cm^2\,s^{-1}$ compared to $D^*_{t,Ar} = 0.0386\,cm^2\,s^{-1}$ and of CS_2 were $D^*_{CS_2} = 0.0263\,cm^2\,s^{-1}$ compared to $D^*_{t,CS_2} = 0.0213\,cm^2\,s^{-1}$. In~~

~~Geba fine sand, coefficients of argon were $D^*_{Ar} = 0.0966\,\mathrm{cm^2\,s^{-1}}$ compared to $D^*_{t,Ar} = 0.0284\,\mathrm{cm^2\,s^{-1}}$ and of CS_2 were $D^*_{CS_2} = 0.0332\,\mathrm{cm^2\,s^{-1}}$ compared to $D^*_{t,CS_2} = 0.0157\,\mathrm{cm^2\,s^{-1}}$.~~ The experimental coefficients D^* differed from the theoretical effective binary diffusion coefficient D^*_t calculated for the prevailing conditions. This could result from the choice of porous media, since both media were characterized by a uniform and narrow grain-size distribution, as well as the observed water-saturation profiles. Werner et al. (2004) reported that theoretical approaches are often sensitive since the majority of their parameters are raised to a high power and do not apply satisfactorily to a wide variety of soils. Furthermore, the theoretical approach does not take into account material characteristics such as the pore-size distribution which may vary for similar porosities and hence affect ~~the tortuosity factor~~ transport. ~~Dispersion coefficients shown in Figure 7 varied for a given velocity due to minor differences between the experiments and to variations arising from the temporal-moment analysis.~~ In addition, the equation used to determine the dispersion coefficient (Eq. A10) from TMA raises the velocity to the power of three, thus minor deviations had a great impact on the final values.

~~The increase in the dispersion coefficient in Figure 7 from the effective binary diffusion coefficient (at $v = 0\,\mathrm{cm\,h^{-1}}$) with increasing velocity resulted from mechanical mixing due to flow through the moist porous medium. This was observed in all experiments. The increase is determined by the slope of the linear regression representing the dispersivity α which should be a parameter of the porous medium only and should be independent of the components (gases) and flow conditions. A slight difference was found between CS_2 and argon for both materials, resulting in a mean dispersivity of $\alpha_{\mathrm{GBfine}} = 0.958\,\mathrm{cm}$ in fine glass beads and $\alpha_{\mathrm{Geba}} = 0.432\,\mathrm{cm}$ in Geba fine sand.~~ The dispersivity α is a parameter of the porous medium only and should be independent of the components (gases) and flow conditions. A mean dispersivity of $\alpha_{\mathrm{GBfine}} = 0.958\,\mathrm{cm}$ in fine glass beads and $\alpha_{\mathrm{Geba}} = 0.432\,\mathrm{cm}$ in Geba fine sand was found. However, a difference between the dispersivity values of argon and CS_2 in the same porous medium was found in the experiments (see Tab. 4) indicating that dispersivity is component dependent, due to ~~Dispersivity may transform from a physical system to a lumped parameter, because of~~ e.g. diffusional or non-equilibrium effects. This ~~then results in a~~ component-dependent dispersivity ~~according to~~ has been shown by Costanza-Robinson and Brusseau (2002a), who reported that dispersivity ranges from approx. 0.1 to 5.0 cm. ~~Since argon is a conservative tracer and CS_2 is affected by retardation, greater reliability was attributed to the dispersivity α_{Ar} determined from BTCs of argon. The results of the experiments in this work demonstrate the impact of seepage velocities on the diffusion/dispersion of CS_2 vapor and of argon. Thus, an influence of the velocity on the retardation of CS_2 was expected.~~ Hence, greater reliability was attributed to the dispersivity α_{Ar} determined from BTCs of argon since it is a conservative tracer.

3.3 Retardation of CS_2

Different series of experiments were conducted to quantify retardation of CS_2 as a function of water saturation and seepage velocity. Figure 8 and 9 compare breakthrough curves (BTC) of argon and CS_2 in dry (black) and moist (red) porous medium for the same seepage velocity ($v = 50\,\mathrm{cm\,h^{-1}}$). Two to three repetitions of each run in dry and moist conditions, respectively, are shown. The graphs show normalized concentrations as a function of effective pore volume (total pore volume minus water content after drainage).

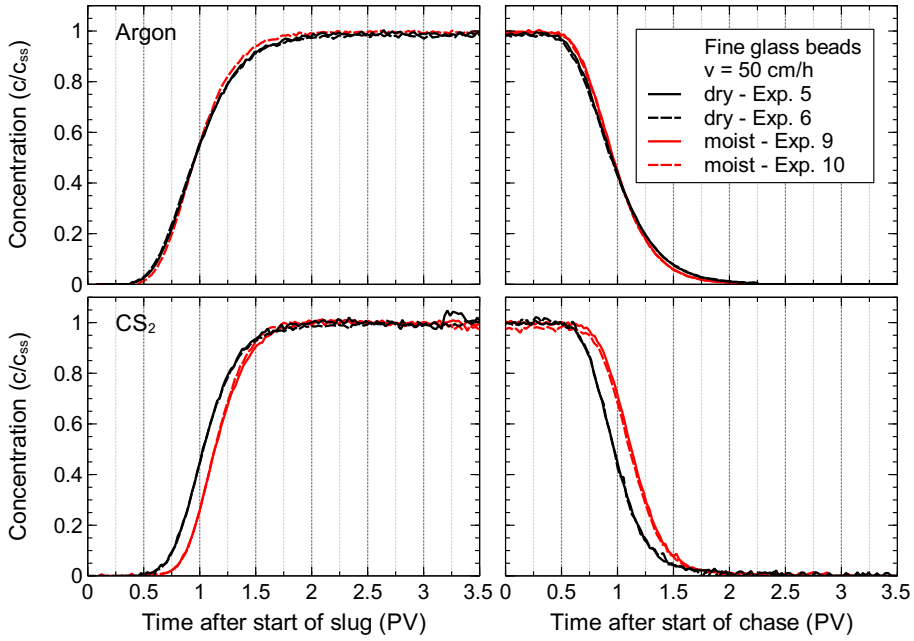

Figure 8. Breakthrough curves of CS_2 and Ar in dry and moist ($S_w = 0.088$) fine glass beads under identical slug and flow conditions (v = 50 cm h^{-1}).

The BTCs of argon showed excellent reproducibility in repetition experiments in both materials at the same conditions ($v = 50\,cm\,h^{-1}$). In fine glass beads, argon showed very similar BTCs for dry and moist experiments. This thus confirmed that argon experiences no retardation and may be used as a conservative tracer and as a reference for CS_2. In Geba fine sand, a different skewness was observed between dry and moist conditions as a result of the reduced pore space in moist conditions. Hence, a comparison of the BTCs revealed that the effective-flow region in fine glass beads was similar in dry and moist conditions, whereas in Geba fine sand it was reduced in moist conditions. This resulted in BTCs which were less affected by diffusion due to a shorter residence time. Since the experiments were conducted with a constant-flow-rate boundary condition based on the calculated effective pore volume, a shorter residence time i.e. higher seepage velocity occurred when the actual effective pore volume available for gas flow is smaller than the calculated volume.

The BTCs of CS_2 showed, in general, good reproducibility for all experiments. In fine glass beads, a later breakthrough of CS_2 compared to argon can be observed in Figure 8, demonstrating the retardation of CS_2 due to partitioning ~~into the water phase~~ processes. The different effective pore volume due to ~~the pore~~ water and possible reduced residence time (actual vs. calculated PV) resulted in less skewed BTCs compared to the dry experiments. In Geba fine sand, a more pronounced retardation of CS_2 was observed compared to experiments in fine glass beads. The later breakthrough becomes evident when comparing BTCs in dry (black) with moist (red) conditions in Figure 9. ~~This could be ascribed to the overall higher water saturation and the increase in saturation toward the bottom of the column (see Fig. 4).~~ In two of the three BTCs in moist experiments (Fig. 9),

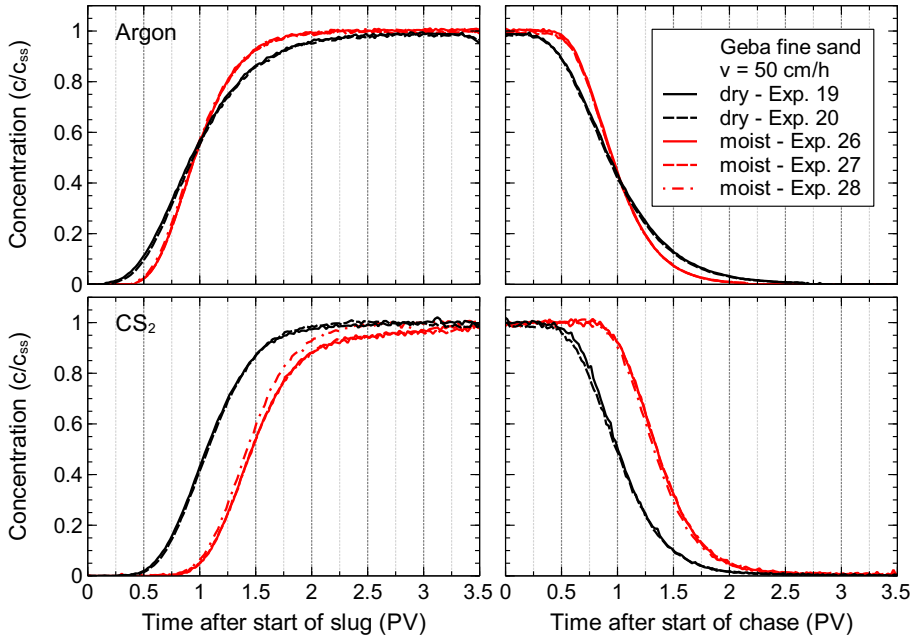

Figure 9. Breakthrough curves of CS_2 and Ar in dry and moist ($S_w = 0.154$) Geba fine sand under identical slug and flow conditions (v = 50 cm h^{-1}).

CS_2 concentrations leveled at around $c/c_{ss} = 0.9$ followed by an increase to steady-state (plateau) concentrations toward the end of the slug. This behavior might be a consequence of the water saturation over column height affecting the partitioning processes.

The retardation coefficients of CS_2 as a function of porous medium, water saturation, and seepage velocity were determined using the temporal-moment analysis (TMA) of the breakthrough curves (see Sec. 2.3). The coefficients were normalized with respect to the BTCs from dry porous medium. Thereby, errors due to set-up or other systematic errors could be eliminated and allowed for the comparison with theoretical values. Figure 10 shows retardation coefficients of CS_2 as a function of water saturation (upper) and seepage velocity (lower) in fine glass beads (black) and Geba fine sand (red). The coefficients of the slug (circle) and the chase (rectangle) are given ~~and their size represents seepage velocity or water saturation~~. Note the broken x-axis (water saturation) between $S_w = 0.10$ and 0.13 in the upper graph indicated by the vertical, dashed lines.

In fine glass beads, a non-linear increase in the retardation coefficient from $R_{GBfine} = 1.09$ to 1.16 with increasing water saturation from $S_w = 0.075$ to 0.155 was observed. ~~Of course, partitioning to the water phase is dependent on the gas-water interfacial area which should decrease with increasing water saturation.~~ Of course, partitioning into the water phase and adsorption to the air–water interface depend on the interfacial area which should decrease with increasing water saturation. Thus an extrapolation of the retardation coefficient to higher water saturations might be difficult. The retardation of the slug and of the chase was different in fine glass beads, the chase being more prone to retardation than the slug. The breakthrough of the

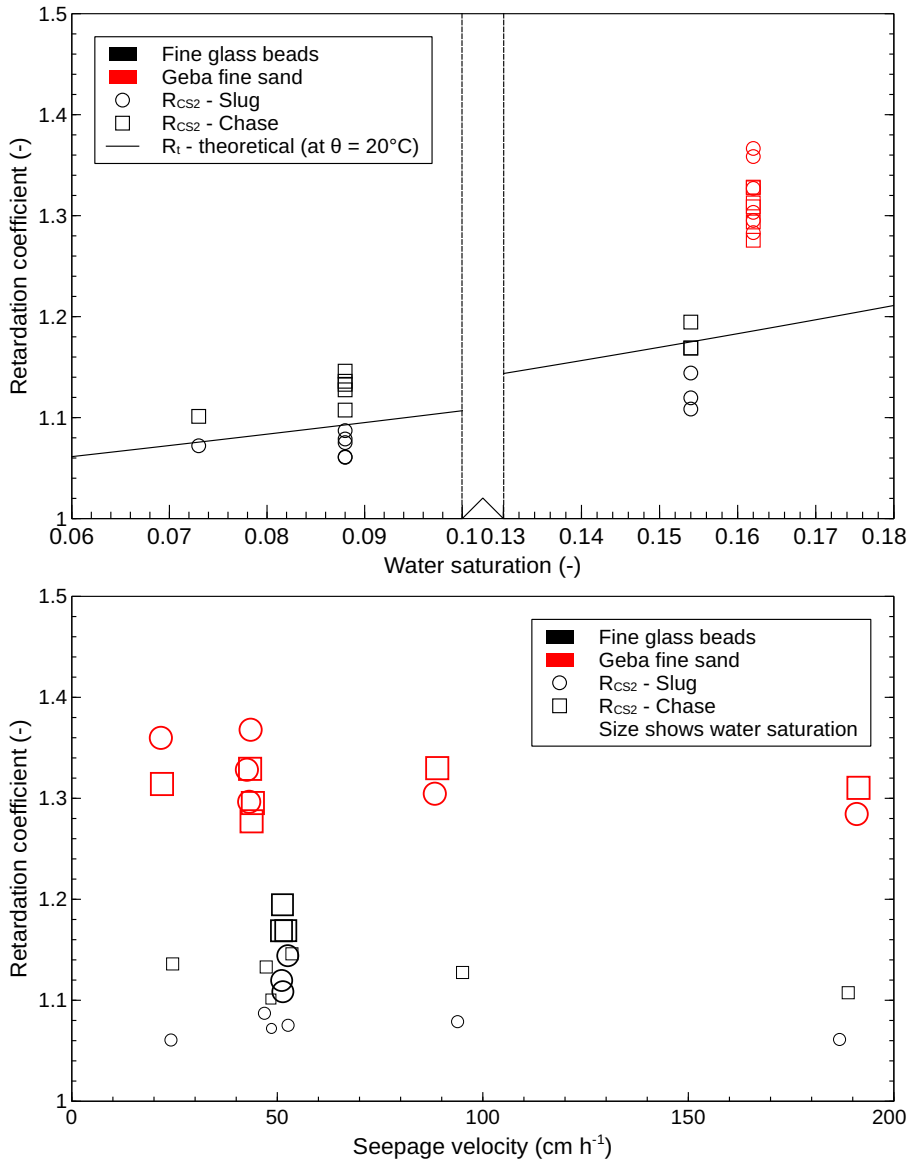

Figure 10. Retardation coefficients of CS_2 determined from experiments with different seepage velocities in fine glass beads and in Geba fine sand at different water saturations (evaluated with temporal-moment analysis).

nitrogen chase (removal of the CS_2 vapor) showed a higher retardation by a factor (average) of 1.05 compared to the break-through of the slug throughout all experiments in fine glass beads. This behavior can be also seen when comparing the BTCs of CS_2 in the upper graph of Figure 8.

In Geba fine sand, higher retardation coefficients compared to fine glass beads were measured in the experiments. These ranged between $R_{Geba} = 1.29$ and 1.34 at a mean water saturation of $S_w = 0.162$. This was due to the higher water saturation and

its increase toward the bottom (discussed in Sec. 3.1), the different gas-water interfacial area, and the pore space available for gas flow. Series 3 in Geba fine sand had to be excluded from these graphs due to mass balance issues discussed later. Hence, results were only available for one particular water saturation profile in Geba fine sand. The ratio between the retardation coefficient of the slug and that of the chase did not show a clear trend as observed in fine glass beads despite the differences seen in Figure 10.

An evaluation of the processes responsible for retardation is possible utilizing the analytical solution (Eq. 2) proposed by Brusseau et al. (1997). The equation includes accumulation in the gas phase, partitioning into the aqueous phase, adsorption to the solid phase, and adsorption to the gas-water interface. Partitioning into the aqueous phase (dissolution) is controlled by the temperature- and component-dependent Henry constant. Since equilibrium is assumed, the relative contribution of this process to the total retardation is considered as maximum.

Adsorption to the solid phase is governed by the partitioning coefficient K_D of that particular component. K_D is the product of the soil organic carbon partitioning coefficient K_{OC} and the fraction of organic carbon in the soil material f_{OC}. According to the Superfund Soil Screening Guidance (USEPA, 1996) for CS_2, the coefficient K_{OC} is 45.7 L kg^{-1}. Howard et al. (1990) reported that "carbon disulfide in solution would therefore not be expected to adsorb significantly to soil" due to the relatively low K_{OC}. The two types of materials used, fine glass beads and Geba fine sand, were evaluated with respect to organic carbon. The chemical composition of fine glass beads (soda-lime glass) is given by the manufacturer (Sigmund Lindner GmbH, SiLibeads Typ S 100 – 200 µm) as SiO_2 (72.5 %), Na_2O (13 %), CaO (9.1 %), MgO (4.2 %), and Al_2O_3 (0.58 %). Geba fine sand (Quarzsande GmbH, Geba weiss, 63 – 350 µm) is composed of SiO_2 (99.2 %), Fe_2O_3 (0.09 %), Al_2O_3 (1.85 %), and TiO_2 (0.24 %), thus a pure quartz sand. Both materials contain negligible fractions of organic carbon (f_{OC}), hence adsorption of CS_2 on the grains did not significantly contribute to retardation and may be neglected.

Adsorption on the air–water interface in a partially water-saturated porous medium depends on the air–water partitioning coefficient K_{IA} and on the air–water interfacial area A_{IA}. The air–water partitioning coefficient K_{IA} of CS_2 was estimated using the empirical correlation (Eq. 4 with Eq. 5) proposed by Valsaraj (1988). This correlation with $log(K_{OW}) = 2.00$ and the dimensionless Henry constant $K_H = 1.04$ yielded the air–water partitioning coefficient of CS_2 $K_{IA} = 6.87 \times 10^{-6} cm$. Costanza-Robinson et al. (2008) found a correlation (Eq. 6) based on on X-ray microtomography measurements of glass beads and natural sands to estimate the interfacial area. The calculated interfacial areas for a water saturation range from 0.05 to 0.20 decreases from 19.5 to 16.4 cm^{-1} for fine glass beads and from 20.9 to 17.5 cm^{-1} for Geba fine sand.

The theoretical retardation coefficient (Eq. 2) as a function of water saturation was calculated based on the assumptions, correlations and parameters discussed above. It is shown as a line in the upper graph of Figure 10. ~~The theoretical coefficient is calculated taking into account the porosity of the porous medium, the water saturation, and the Henry coefficient. Hence, only one function is shown in the upper graph of Figure 10, since the porosities of the fine glass beads and the Geba fine sand used were similar.~~ Only one line is plotted for both materials as the results are nearly identical due to similar porosities and calculated interfacial areas. In fine glass beads, the theoretical coefficient compared very well with the values from the experiments. It slightly overpredicted the retardation of the slug while it underpredicted that of the chase, however it reproduced satisfactorily the mean retardation coefficient and its increase with water saturation. In Geba fine sand, the theoretical coefficient, taking into

account dissolution and adsorption to the air–water interface, significantly underestimated the observed retardation. The ratio between the contributions from dissolution β_w and from air–water interfacial adsorption β_{IA} at $S_w = 0.162$ yields $\beta_w/\beta_{IA} = 513$. Since dissolution, which is a function of the Henry constant and assumes equilibrium, is already at its maximum and adsorption to the grains may be neglected as discussed above, it is postulated that this increased retardation can only be caused by air–water interfacial adsorption. Possible reasons for an underestimation of the adsorption to the air–water interface could be that the inhomogeneous water saturation profiles (see Fig. 4), the grain-size distribution, or the underestimation of the specific surface of the Geba fine sand particles lead to an underestimation of the interfacial area. Scanning electron microscopy images (Fig. 3) suggested that the smooth-sphere assumption holds for glass beads but not necessarily for Geba fine sand, thus the interfacial area for Geba fine sand might have been significantly underestimated. Interfacial areas measured with microtomography are smaller than those determined with vapor-phase tracer experiments (Brusseau et al., 2006; Costanza-Robinson et al., 2008). Furthermore, they reported that A_{IA} from microtomography measurements approach a maximum value similar to the smooth-sphere assumption while measurements from vapor-phase experiments rather approach a maximum close to the specific surface area of the material (BET measurements) as water saturation approaches zero. Costanza et al. (2000) observed the maximum interfacial area for water saturation in the range of 15 to 25 %. They also reported the possibility of multilayer adsorption and that the actual adsorption may be significantly underestimated when true A_{IA} values are used.

Attributing the observed discrepancy in Geba fine sand to air–water interfacial adsorption of CS_2, an interfacial area of about $A_{IA,calc} = 6553\ cm^{-1}$ would be required to obtain a mean retardation factor of $R_{Geba} = 1.31$. This is consistent with measured interfacial areas from vapor-phase tracer experiments (e.g. Costanza et al., 2000). Further experiments would be required using an additional tracer for air–water interfacial adsorption to actually measure the area and thereby quantify the relative contribution of dissolution and interfacial adsorption to the total retardation of CS_2. ~~The findings suggest that retardation may vary along the depth of the unsaturated zone due to spatially-varying water saturations and especially around the capillary fringe in the vicinity of the groundwater level.~~ The findings suggest that retardation may vary with changing saturation as a function of distance from groundwater table due to varying relative contributions of the partitioning processes. Since water saturations increase toward the groundwater table, more contaminant mass can partition into the bulk water phase but less mass is adsorbed to the air-water interface due to a reduced interfacial area.

~~The experiments were conducted with different seepage velocities to evaluate their impact on retardation.~~ The lower graph in Figure 10 shows the retardation coefficients as a function of seepage velocity. A mean retardation coefficient of $R_{GBfine} = 1.100 \pm 0.0096$ and $R_{Geba} = 1.315 \pm 0.0152$ was measured in the experiments with fine glass beads ($S_w = 0.088$) and Geba fine sand ($S_w = 0.162$), respectively. In general, no significant change of the retardation behavior with increasing seepage velocity was observed. This confirmed that the mass transport rate was low enough and the residence time of the slug was sufficient for the partitioning processes to reach equilibrium. Concluding from the experiment with $v = 200\ \mathrm{cm\ h^{-1}}$ it seems likely that there was a slight tendency toward a reduced retardation. In fact, retardation may reduce at higher seepage velocities due to limiting contaminant diffusion. If no equilibrium is reached in case of high velocities, the retardation coefficient reflects an apparent coefficient since in this case it is a function of the experimental system used (i.e. length of the column). Additional experimental repetitions would have been required to provide proof. However, this experimental investigation aimed at characterizing

retardation of CS_2 in the range of ~~seepage~~ velocities observed during vapor-plume migration experiments ($v \ll 200\,cm\,h^{-1}$). Hence, the focus was laid on the velocities used and higher values were beyond the scope.

Mass balance analyses were performed to obtain mass recovery (r) from each breakthrough curve. Mass recovery was calculated from concentration and flow measurements and was normalized with respect to the injected mass. In general, mass recoveries of argon and CS_2 showed good results. ~~The mean recovery of argon calculated from all vapor-retardation experiments conducted (excluding experiments of Series 3) yielded $r_{Ar} = 0.995 \pm 0.007$ and confirmed complete mass recovery. The mean recovery of CS_2 was $r_{CS_2} = 0.981 \pm 0.084$, thus only suggesting slight mass losses.~~ Mean recovery calculated from all experiments conducted yielded for argon $r_{Ar} = 0.995 \pm 0.007$ and for CS_2 $r_{CS_2} = 0.981 \pm 0.084$ (excluding experiments of Series 3). Mass recoveries of all experiments are given in Tables 5 and 6 in the appendix. ~~The mass balance and complete recovery~~ Complete mass recoveries proved reliability and quality of the results gained from these column experiments.

The results discussed above excluded Series 3 in Geba fine sand. Series 3 ~~was~~ referred to the second saturation and drainage cycle which was carried out to establish a static water saturation different than in Series 2. However, significant CS_2 mass losses were observed and became more pronounced with each experiment in this series, eventually leading to its exclusion from the results. Recoveries of CS_2 decreased from $r_{CS_2} = 0.854$ in the first experiment of Series 3 down to $r_{CS_2} = 0.010$. This mass loss of CS_2 was caused by biodegradation which was confirmed by the smell of hydrogen sulfide in the column outflow. ~~Cox et al. (2013) found carbonyl sulfide (COS) and hydrogen sulfide (H_2S) as by-products during CS_2 biodegradation in their experiments.~~ The mass balance analysis of the experiments enabled for determining mean degradation rates of CS_2 which were calculated from the CS_2 mass rate and the recovery. The mean degradation rates ranged from 0.12 to $1.28\,mg\,h^{-1}$ depending on the ~~respective seepage velocity~~ CS_2 mass flux applied in the experiments. Microbial degradation of CS_2 under aerobic and anaerobic conditions has been studied in the field of waste-gas treatment (e.g. Smith and Kelly, 1988; Hartikainen et al., 2000; Pol et al., 2007). They found microbes of the Thiobacillus species able to oxidize CS_2 under certain conditions. Cox et al. (2013) were the first to study degradation in soils and groundwater from a CS_2-contaminated site. They confirmed carbonyl sulfide (COS) and hydrogen sulfide (H_2S) as by-products and reported almost 100 % CS_2 degradation due to biological activity in their soil experiments. However, they also found evidence for microbial self-inhibition with increasing CS_2 concentration. This has been also reported by Pol et al. (2007) who additionally found inhibition of degradation due to accumulation of the intermediate products COS and H_2S. Hence, biodegradation is only relevant in specific environments and conditions and is most likely reduced as concentrations increase closer to the source zone of a contaminated site. This may explain why CS_2 is still persistent at many of the NPL sites listing CS_2 as a contaminant of concern.

A direct comparison with reported degradation rate constants determined from batch experiments could not be achieved due to the only availability of effluent gas concentrations in our experiments. Nonetheless, they showed that biodegradation may have a considerable potential for mitigating the contaminant mass transfer by vapor migration to the underlying aquifer, provided that favorable conditions for the specific microbes can be ensured, for instance via soil venting. A detailed investigation of biodegradation was beyond the scope of this work but should be addressed in future research.

4 Conclusions

- The retardation of CS_2 vapor was quantified in 2 m long column experiments in two different porous media as a function of ~~porous medium,~~ water saturation, and ~~seepage~~ velocity by comparison with the conservative tracer argon. ~~The novel set-up and methods applied additionally allowed for characterizing the transport of CS_2 and argon.~~ The temporal-moment analysis for a step-input (TMA) was applied to determine retardation factors and dispersion coefficients from concentration breakthrough curves. Comparison between experiments was achieved by relating mean arrival times of CS_2 to these of argon.

- ~~The versatile temporal-moment analysis (TMA) was successfully applied to quantify diffusion/dispersion of CS_2 and argon as well as retardation of CS_2 from concentration breakthrough curves by comparison with the conservative tracer argon.~~

- ~~Dispersion coefficients as a function of seepage velocity were obtained from the TMA for experiments in moist conditions. Linear regressions of these data sets yielded effective binary dispersion coefficients and dispersivity values at the prevailing experimental conditions. The effective binary diffusion coefficient at the given experimental conditions was found to be slightly higher than theoretical values based on the approach by Millington and Quirk (1961). The theoretical approach takes into account the porosity only and neglects material characteristics such as grain-size or pore-size distribution which affect diffusion/dispersion. Thus, the experiments confirm that theoretical approaches do not satisfactorily apply to a wide variety of porous media (Werner et al., 2004).~~

- ~~The impact of different seepage velocities on the breakthrough curves and thus on the dispersion coefficient was observed. The experiments showed that the velocities affected diffusion/dispersion of the gases due to the corresponding residence time in the porous medium and due to mechanical mixing. This effect was illustrated by the skewness of the breakthrough curves which were negatively correlated to the seepage velocity.~~

- ~~The retardation coefficient of CS_2 increased with increasing water saturation and compared very well with the theoretical approach for fine glass beads.~~ The retardation coefficient of CS_2 increased from around 1.08 to 1.14 with increasing water saturation from 0.073 to 0.154 in fine glass beads. A slightly higher retardation of the chase by a factor of 1.05 compared to that of the slug was observed. A pronounced higher mean retardation of 1.31 was observed in Geba fine sand and a water saturation of 0.162 due to the different grain-size distribution and the particular water-saturation profile. Retardation coefficients as a function of (seepage) velocity revealed only a minor dependency and suggested a slight tendency toward a reduced retardation at higher velocities.

- The experimental retardation coefficients were compared to an analytical solution considering accumulation in the gas phase, partitioning to the aqueous phase, and adsorption to the air–water interface. Adsorption to the solid phase was neglected due to negligible fractions of organic matter in the porous media used. The analytic solution compared very well with the experimental results in fine glass beads identifying dissolution as the main contribution to retardation.

However, it underpredicted retardation in Geba fine sand. The discrepancy was ascribed to an increased relative contribution of air–water interfacial adsorption in Geba fine sand as a result of a significant underestimation of the interfacial area. They were estimated using a correlation derived from microtomography measurements of glass beads and natural soils and utilizing the smooth-sphere assumption (Costanza-Robinson et al., 2008). A readily applicable correlation to estimate interfacial areas is still considered a challenge and vapor-phase tracer experiments are so far the only reliable method to measure effective interfacial areas for vapor retardation. A quantification of the effective interfacial area could be achieved by using additional tracers which predominantly adsorb to the air–water interface.

- Clear evidence of the biodegradation of CS_2 was found in the last series of experiments in Geba fine sand confirmed by the concentration measurements and the mass balance analysis. These findings demonstrate the potential of biodegradation to reduce the total CS_2 mass ~~in case of a contamination in the unsaturated zone and~~ of migrating vapor plumes eventually threating the underlying aquifer. Biodegradation of CS_2 has been confirmed by several experimental studies (e.g. Pol et al., 2007; Cox et al., 2013), however they showed that CS_2 degradation is only relevant in specific environments and conditions due to microbial self-inhibition at higher concentrations. Thus, site-specific investigations are needed to evaluate the potential for biodegradation or natural attenuation of a CS_2 contamination. Soil venting could be used to reduce self-inhibition and enhance biodegradation.

- ~~The experiments conducted clearly proved that a migrating CS_2-vapor plume in the unsaturated zone is retarded and that dissolved CS_2 is amenable to biodegradation. The breakthrough of the slug and of the chase was observed and evaluated, the latter demonstrating a complete removal of the gaseous CS_2 confirmed by mass balance analyses.~~ The experiments showed a complete removal of the CS_2 vapor and a reversibility of partitioning processes confirmed by mass balance analyses. Vaporization rates of liquid CS_2 were not studied in this work and need to be investigated to estimate the removal efficiency of a liquid spill. Nevertheless a fast vaporization of liquid CS_2 is expected due to its low boiling point and high vapor pressure. This clearly supports the remediation of a ~~liquid~~ CS_2 ~~spill~~ contamination in the unsaturated zone using soil-vapor extraction.

Data availability

The experimental data used to produce the results and graphs presented in this manuscript is available at http://dx.doi.org/10.4228/ZALF.2013.295 (Kleinknecht, 2016).

Appendix A: Materials and methods

A1 Binary diffusion coefficient

The Chapman-Enskog formula is used to estimate the binary diffusion coefficient of component A in B at low density.

$$D_{AB} = 1.8583 \times 10^{-3} \frac{\sqrt{T^3 \left(\frac{1}{M_A} + \frac{1}{M_B}\right)}}{p\sigma_{AB}^2 \Omega_{D,AB}} \tag{A1}$$

with D_{AB} (cm^2 s^{-1}), temperature T (K), pressure p (atm), the Lennard-Jones parameter σ_{AB} (angstrom), and the collision integral $\Omega_{D,AB}$ which can be approximated with the Lennard-Jones potential. Component-specific values to determine σ_{AB} as well as $\Omega_{D,AB}$ as a function of kT/ϵ can be found in Bird et al. (1960).

Porous media affect diffusion of gases since space is occupied by grains and possibly by additional fluid phases. Therefore, Fick's law is often modified by the factor β to account for these deviations.

$$D^* = \beta D_{AB} \tag{A2}$$

while β is defined as

$$\beta = \phi S_g \tau \tag{A3}$$

where D_{AB}^* is the effective diffusion coefficient in porous media, ϕ is the porosity, S_g the gas saturation (equal to 1 for all-gas condition), and τ is the tortuosity. According to Millington and Quirk (1961), tortuosity can be approximated by

$$\tau = \phi^{1/3} S_g^{7/3} \tag{A4}$$

A2 Dispersion coefficient

Flow of fluids in a porous medium may vary significantly on a micro scale due to the velocity field in pores, irregularities of the pore size, flow restrictions, or dead-end pores resulting in additional spreading denoted as dispersion. These influences have to be taken into account in analytical or numerical solutions of flow in porous media. This is done by introducing the longitudinal dispersion coefficient

$$D = \beta D_{AB} + \alpha v = D^* + \alpha v \tag{A5}$$

with the dispersion coefficient D (cm^2 s^{-1}), effective binary diffusion coefficient D_{AB}^* (cm^2 s^{-1}) according to Eq. A2, gas-phase longitudinal dispersivity α (cm), and average gas velocity v (cm s^{-1}).

A3 Temporal-moment analysis

The measured breakthrough curve (BTC) data had to be prepared to allow for the usage of the temporal-moment analysis (TMA) generally applied to responses from dirac input. The breakthrough curves of the step-input boundary condition (1)

were transformed to a dirac-input boundary condition (2) (Yu et al., 1999). This was achieved by using the derivative of the original step-input BTC data.

$$\frac{\partial c_1}{\partial t} = c_2 \tag{A6}$$

This transformation then allowed for analyzing the original breakthrough curves and required adapted definitions of the temporal moments. The first order normalized moment M_1 representing the mean breakthrough arrival time (τ) is then defined as

$$\tau = M_1 = \frac{m_1}{m_0} = \frac{\int_0^1 t\, dc_1}{\int_0^1 dc_1}, \tag{A7}$$

where c_1 (-) is normalized concentration of measured BTC and t (second or PV) is elapsed time. The second central moment μ_2 corresponds to the variance of travel times at the location of measurement and is given by

$$\mu_2 = \int_0^1 (t - M_1)^2\, dc_1. \tag{A8}$$

These two moments can be used to directly infer seepage velocity v and dispersion coefficient D from BTC data for a one-dimensional system (Cirpka and Kitanidis, 2000).

$$v = \frac{z}{M_1} \tag{A9}$$

$$D = \frac{\mu_2 v^3}{2z} \tag{A10}$$

Appendix B: Detailed experimental results

Tables 5 and 6 show the theoretical seepage velocity, the injection duration (slug), the injected mass, and the normalized recovery of the components CS_2 and argon. The tables list all experiments in order according to the conducted series.

Author contributions. Simon M. Kleinknecht designed and conducted this experimental study. Holger Class and Jürgen Braun were responsible for the scientific and experimental supervision. Simon M. Kleinknecht prepared the manuscript with contributions from both co-authors. The authors declare that they have no conflict of interest.

Table 5. Experimental conditions of vapor-retardation experiments in fine glass beads: series, experiment, theoretical seepage velocity, injection duration, and injected mass and recovery of CS_2 and argon.

Series	Exp.	v	t_{inj}	m_{Ar}	m_{CS2}	r_{Ar}	r_{CS2}
#	#	$cm\,h^{-1}$	h	mg	mg	-	-
Fine glass beads							
1	1	25	27.80	667.8	2671.4	0.994	1.123
	2	50	13.92	677.7	2710.9	1.011	1.066
	3	50	14.10	675.9	2703.5	0.996	1.005
	4	50	13.65	677.7	542.2	0.992	1.033
	5	50	14.29	690.3	13.8	0.988	0.822
	6	50	14.07	687.0	13.7	0.984	0.753
	7	50	13.82	673.3	13.5	0.987	0.770
2	8	25	28.35	619.9	12.4	0.989	1.022
	9	50	14.40	617.8	12.4	0.993	0.983
	10	50	12.83	615.2	12.3	0.997	1.010
	11	100	7.22	620.8	12.4	1.000	0.941
	12	200	3.56	617.1	12.3	0.998	0.941
3	13	50	14.38	635.0	12.7	0.995	1.054
	14	50	14.22	634.0	12.7	1.000	1.032
	15	50	14.43	635.4	12.7	0.989	1.013
4	16	50	14.06	626.0	12.5	0.994	1.039

Table 6. Experimental conditions of vapor-retardation experiments in Geba fine sand: series, experiment, theoretical seepage velocity, injection duration, and injected mass and recovery of CS_2 and argon.

Series	Exp.	v	t_{inj}	m_{Ar}	m_{CS2}	r_{Ar}	r_{CS2}
#	#	cm h^{-1}	h	mg	mg	-	-
Geba fine sand							
1	17	25	28.71	673.9	13.5	0.982	0.964
	18	25	40.97	944.5	18.9	0.992	0.942
	19	50	14.30	599.2	12.0	0.985	1.006
	20	50	14.31	597.5	12.0	0.983	0.970
	21	100	7.20	664.8	13.3	0.999	0.994
	22	100	7.32	665.9	13.3	0.999	1.062
	23	200	3.83	706.2	14.1	1.000	0.994
	24	200	3.54	657.7	13.2	0.995	0.962
2	25	25	41.17	795.7	15.9	0.984	1.009
	26	50	14.33	552.8	11.1	1.000	0.955
	27	50	20.28	767.3	15.3	0.992	1.115
	28	50	20.62	799.5	16.0	0.997	0.973
	29	100	10.12	797.6	16.0	0.987	0.965
	30	200	4.67	800.8	16.0	1.000	1.013
3	31	50	20.54	815.8	16.3	0.994	0.854
	32	50	24.04	955.8	19.1	0.998	0.684
	33	100	11.02	864.1	17.3	1.000	0.534
	34	200	5.16	782.9	15.7	1.008	0.689
	35	25	49.26	957.3	19.1	1.012	0.010
	36	100	10.28	793.0	15.9	1.000	0.174
	37	50	23.81	944.0	18.9	0.996	0.016

References

Barber, C. and Davis, G. B.: Fugacity model to assess the importance of factors controlling the movement of volatile organics from soil to ground water, in: Proceedings of a Workshop on Modelling the Fate of Chemicals in the Environment, pp. 67–73, The Australian National University, Centre for Resource and Environmental Studies, Water Research Foundation of Australia, 1991.

Bird, R. B., Stewart, W. E., and Lightfoot, E. N.: Transport phenomena, Wiley, New York, 1960.

Brusseau, M. L., Popovičová, J., and Silva, J. A. K.: Characterizing gas-water interfacial and bulk-water partitioning for gas-phase transport of organic contaminants in unsaturated porous media, Environmental Science & Technology, 31, 1645–1649, doi:10.1021/es960475j, 1997.

Brusseau, M. L., Peng, S., Schnaar, G., and Costanza-Robinson, M. S.: Relationships among air-water interfacial area, capillary pressure, and water saturation for a sandy porous medium, Water Resources Research, 42, n/a–n/a, doi:10.1029/2005WR004058, http://dx.doi.org/10.1029/2005WR004058, w03501, 2006.

Brusseau, M. L., Carroll, K. C., Truex, M. J., and Becker, D. J.: Characterization and Remediation of Chlorinated Volatile Organic Contaminants in the Vadose Zone, Vadose Zone Journal, 12, –, doi:10.2136/vzj2012.0137, http://dx.doi.org/10.2136/vzj2012.0137, 2013.

Brusseau, M. L., Ouni, A. E., Araujo, J. B., and Zhong, H.: Novel methods for measuring air–water interfacial area in unsaturated porous media, Chemosphere, 127, 208 – 213, doi:http://dx.doi.org/10.1016/j.chemosphere.2015.01.029, http://www.sciencedirect.com/science/article/pii/S0045653515000697, 2015.

Budavari, S., ed.: The Merck index: an encyclopedia of chemicals, drugs, and biologicals, Merck, Whitehouse Station, NJ, 12. edn., http://www.gbv.de/dms/ohb-opac/198126255.pdf, 1996.

Cabbar, H. and Bostanci, A.: Moisture effect on the transport of organic vapors in sand, Journal of Hazardous Materials, 82, 313–322, doi:10.1016/S0304-3894(01)00177-7, http://www.sciencedirect.com/science/article/pii/S0304389401001777, 2001.

Cirpka, O. A. and Kitanidis, P. K.: Characterization of mixing and dilution in heterogeneous aquifers by means of local temporal moments, Water Resources Research, 36, 1221–1236, doi:10.1029/1999WR900354, http://dx.doi.org/10.1029/1999WR900354, 2000.

Corley, T. L., Farrell, J., Hong, B., and Conklin, M. H.: VOC accumulation and pore filling in unsaturated porous media, Environmental Science & Technology, 30, 2884–2891, doi:10.1021/es950644k, 1996.

Costanza, M. S., , and Brusseau, M. L.: Contaminant Vapor Adsorption at the Gas–Water Interface in Soils, Environmental Science & Technology, 34, http://pubs.acs.org/doi/abs/10.1021/es9904585, 2000.

Costanza-Robinson, M. S. and Brusseau, M. L.: Gas phase advection and dispersion in unsaturated porous media, Water Resources Research, 38, 7–1–7–9, doi:10.1029/2001WR000895, 2002a.

Costanza-Robinson, M. S. and Brusseau, M. L.: Air-water interfacial areas in unsaturated soils: Evaluation of interfacial domains, Water Resour. Res., 38, 13–1–13–17, http://dx.doi.org/10.1029/2001WR000738, 2002b.

Costanza-Robinson, M. S., Harrold, K. H., and Lieb-Lappen, R. M.: X-ray Microtomography Determination of Air–Water Interfacial Area–Water Saturation Relationships in Sandy Porous Media, Environ. Sci. Technol., 42, 2949–2956, doi:10.1021/es072080d, http://pubs.acs.org/doi/abs/10.1021/es072080d, 2008.

Costanza-Robinson, M. S., Carlson, T. D., and Brusseau, M. L.: Vapor-phase transport of trichloroethene in an intermediate-scale vadose-zone system: Retention processes and tracer-based prediction, Journal of Contaminant Hydrology, 145, 82–89, doi:10.1016/j.jconhyd.2012.12.004, http://www.sciencedirect.com/science/article/pii/S0169772212001696, 2013.

Cox, S. F., McKinley, J. D., Ferguson, A. S., O'Sullivan, G., and Kalin, R. M.: Degradation of carbon disulphide (CS2) in soils and groundwater from a CS2-contaminated site, Environmental Earth Sciences, 68, 1935–1944, doi:10.1007/s12665-012-1881-y, http://dx.doi.org/10.1007/s12665-012-1881-y, 2013.

Davis, A., Fennemore, G., Peck, C., Walker, C., McIlwraith, J., and Thomas, S.: Degradation of carbon tetrachloride in a reducing groundwater environment: implications for natural attenuation, Applied Geochemistry, 18, 503 – 525, doi:http://dx.doi.org/10.1016/S0883-2927(02)00102-6, http://www.sciencedirect.com/science/article/pii/S0883292702001026, 2003.

Davis, G., Patterson, B., and Trefry, M.: Evidence for Instantaneous Oxygen-Limited Biodegradation of Petroleum Hydrocarbon Vapors in the Subsurface, Ground water monitoring & remediation, 29, 126–137, doi:10.1111/j.1745-6592.2008.01221.x, 2009.

Davis, G. B., Rayner, J. L., Trefry, M. G., Fisher, S. J., and Patterson, B. M.: Measurement and modeling of temporal variations in hydrocarbon vapor behavior in a layered soil profile, Vadose Zone Journal, 4, 225–239, doi:10.2136/vzj2004.0029, https://dl.sciencesocieties.org/publications/vzj/abstracts/4/2/225, 2005.

for Toxic Substances, A. and Registry, D.: Priority List of Hazardous Substance, https://www.atsdr.cdc.gov/spl/, 2015.

Goss, K.-U.: Predicting Adsorption of Organic Chemicals at the Air−Water Interface, The Journal of Physical Chemistry A, 113, 12 256–12 259, doi:10.1021/jp907347p, pMID: 19803507, 2009.

Hartikainen, T., Ruuskanen, J., Räty, K., von Wright, A., and Martikainen, P.: Physiology and taxonomy of Thiobacillus strain TJ330, which oxidizes carbon disulphide (CS2), Journal of Applied Microbiology, 89, 580–586, doi:10.1046/j.1365-2672.2000.01150.x, 2000.

Hoff, J. T., Gillham, R., Mackay, D., and Shiu, W. Y.: Sorption of organic vapors at the air-water interface in a sandy aquifer material, Environmental Science & Technology, 27, 2789–2794, doi:10.1021/es00049a018, 1993.

Höhener, P., Dakhel, N., Christophersen, M., Broholm, M., and Kjeldsen, P.: Biodegradation of hydrocarbons vapors: comparison of laboratory studies and field investigations in the vadose zone at the emplaced fuel source experiment, Airbase Værløse, Denmark, Journal of Contaminant Hydrology, 88, 337–358, doi:10.1016/j.jconhyd.2006.07.007, http://www.sciencedirect.com/science/article/pii/S0169772206001343, 2006.

Howard, P., Sage, G., Jarvis, W., and Gray, D.: Handbook of environmental fate and exposure data for organic chemicals. Volume II: Solvents, Chelsea, MI (US); Lewis Publishers, Inc., 1990.

Kibbey, T. C. G. and Chen, L.: A pore network model study of the fluid-fluid interfacial areas measured by dynamic-interface tracer depletion and miscible displacement water phase advective tracer methods, Water Resources Research, 48, n/a–n/a, doi:10.1029/2012WR011862, http://dx.doi.org/10.1029/2012WR011862, w10519, 2012.

Kim, H., Rao, P. S. C., and Annable, M. D.: Determination of effective air-water interfacial area in partially saturated porous media using surfactant adsorption, Water Resources Research, 33, 2705–2711, doi:10.1029/97WR02227, 1997.

Kim, H., Annable, M. D., and Rao, P. S. C.: Influence of air-water interfacial adsorption and gas-phase partitioning on the transport of organic chemicals in unsaturated porous media, Environmental Science & Technology, 32, 1253–1259, doi:10.1021/es970868y, 1998.

Kleinknecht, S.: Data sets of experimental study on retardation of a heavy NAPL vapor in partially saturated porous media, Leibniz-Zentrum für Agrarlandschaftsforschung (ZALF) e.V., doi:10.4228/ZALF.2013.295, 2016.

Kleinknecht, S. M., Class, H., and Braun, J.: Density-driven migration of heavy NAPL vapor in the unsaturated zone, Vadose Zone Journal, 14, doi:10.2136/vzj2014.12.0173, http://dx.doi.org/10.2136/vzj2014.12.0173, 2015.

Lagioia, R., Sanzeni, A., and Colleselli, F.: Air, water and vacuum pluviation of sand specimens for the triaxial apparatus, Soils And Foundations, 46, 61–67, doi:10.3208/sandf.46.61, 2006.

Lide, D. R.: CRC Handbook of chemistry and physics, CRC Press, 86 edn., 2005.

Luo, J., Cirpka, O. A., and Kitanidis, P. K.: Temporal-moment matching for truncated breakthrough curves for step or step-pulse injection, Advances in Water Resources, 29, 1306–1313, doi:10.1016/j.advwatres.2005.10.005, http://www.sciencedirect.com/science/article/pii/S0309170805002496, 2006.

Maxfield, B. T., Ginosar, D. M., McMurtrey, R. D., Rollins, H. W., and Shook, G. M.: The effect of moisture content on retention of fluorocarbon tracers on sand, Geothermics, 34, 47–60, doi:10.1016/j.geothermics.2004.06.003, http://www.sciencedirect.com/science/article/pii/S0375650504000392, 2005.

Mayes, M., Jardine, P., Mehlhorn, T., Bjornstad, B., Ladd, J., and Zachara, J.: Transport of multiple tracers in variably saturated humid region structured soils and semi-arid region laminated sediments, Journal of Hydrology, 275, 141–161, doi:10.1016/S0022-1694(03)00039-8, http://www.sciencedirect.com/science/article/pii/S0022169403000398, 2003.

McGeough, K. L., Kalin, R. M., and Myles, P.: Carbon disulfide removal by zero valent iron, Environmental Science & Technology, 41, 4607–4612, doi:10.1021/es062936z, 2007.

Millington, R. J. and Quirk, J. P.: Permeability of porous solids, Transactions of the Faraday Society, 57, 1200–1207, doi:10.1039/TF9615701200, 1961.

Pol, A., van der Drift, C., and Op den Camp, H.: Isolation of a carbon disulfide utilizing Thiomonas sp. and its application in a biotrickling filter, Applied Microbiology and Biotechnology, 74, 439–446, doi:10.1007/s00253-006-0663-4, 2007.

Popovičová, J. and Brusseau, M. L.: Contaminant mass transfer during gas-phase transport in unsaturated porous media, Water Resources Research, 34, 83–92, doi:10.1029/97WR02945, 1998.

Rad, N. and Tumay, M.: Factors affecting sand specimen fabrication by raining, Geotechnical Testing Journal, 10, 31–37, doi:10.1520/GTJ10136J, 1987.

Riddick, J. A., Bunger, W. B., and Sakano, T. K.: Organic Solvents: Physical Properties And Methods Of Purification, vol. XV, Wiley, New York, 4th edn., http://www.gbv.de/dms/ilmenau/toc/01792670X.PDF, 1986.

Rivett, M. O., Wealthall, G. P., Dearden, R. A., and McAlary, T. A.: Review of unsaturated-zone transport and attenuation of volatile organic compound (VOC) plumes leached from shallow source zones, Journal of Contaminant Hydrology, 123, 130–156, doi:10.1016/j.jconhyd.2010.12.013, http://www.sciencedirect.com/science/article/B6V94-51XH94M-1/2/000e9c8578e4476286054f5b05ca15e4, 2011.

Smith, N. A. and Kelly, D. P.: Oxidation of Carbon Disulphide as the Sole Source of Energy for the Autotrophic Growth of Thiobacillus thioparus Strain TK-m, Microbiology, 134, 3041–3048, http://mic.microbiologyresearch.org/content/journal/micro/10.1099/00221287-134-11-3041, 1988.

Toride, N., Inoue, M., and Leij, F. J.: Hydrodynamic dispersion in an unsaturated dune sand, Soil Science Society of America Journal, 67, 703–712, doi:10.2136/sssaj2003.0703, https://www.soils.org/publications/sssaj/abstracts/67/3/703, 2003.

U.S. Environmental Protection Agency: Superfund Soil Screening Guidance – Technical Background Document – Part 5: Chemical-Specific Parameters, Tech. rep., Office of Solid Waste and Emergency Response, https://semspub.epa.gov/work/HQ/175235.pdf, 1996.

U.S. Environmental Protection Agency: National Priority List (NPL): advanced query form, https://cumulis.epa.gov/supercpad/cursites/srchsites.cfm, 2016.

Valsaraj, K. T.: On the physico-chemical aspects of partitioning of non-polar hydrophobic organics at the air-water interface, Chemosphere, 17, 875 – 887, doi:http://dx.doi.org/10.1016/0045-6535(88)90060-4, http://www.sciencedirect.com/science/article/pii/0045653588900604, 1988.

Werner, D., Grathwohl, P., and Höhener, P.: Review of field methods for the determination of the tortuosity and effective gas-phase diffusivity in the vadose zone, Vadose Zone Journal, 3, 1240–1248, doi:10.2136/vzj2004.1240, http://dx.doi.org/10.2136/vzj2004.1240, 2004.

Yu, C., Warrick, A. W., and Conklin, M. H.: A moment method for analyzing breakthrough curves of step inputs, Water Resources Research, 35, 3567–3572, doi:10.1029/1999WR900225, http://dx.doi.org/10.1029/1999WR900225, 1999.